Neuroradiology (2000) 42: 471–491

P. Tortori-Donati
A. Rossi
A. Cama

Spinal dysraphism: a review of neuroradiological features with embryological correlations and proposal for a new classification

Received: 6 December 1999
Accepted: 27 December 1999

P. Tortori-Donati (✉) · A. Rossi
Department of Paediatric Neuroradiology,
G. Gaslini Children's Research Hospital,
Largo G. Gaslini 5, 16147 Genova,
Italy
e-mail: tortori@panet.it
Tel.: + 39 10 5636618
Fax: + 39 10 3779798

A. Cama
Department of Paediatric Neurosurgery,
G. Gaslini Children's Research Hospital,
Genova, Italy

Abstract Our purpose was to review the neuroradiological features of spinal dysraphism and to correlate them with clinical findings and up-to-date embryological theory. We also aimed to formulate a working classification which might prove useful in clinical practice. We reviewed series of 986 children referred to our Spina Bifida Centre in the past 24 years. There were 353 children with open spinal (OSD) and 633 with closed (skin-covered) spinal (CSD) dysraphism. By far the most common open abnormality was myelomeningocele, and all patients with OSD had a Chiari II malformation. CSD was categorised clinically, depending on the presence of a subcutaneous mass in the back. CSD with a mass mainly consisted of lipomas with dural defects and meningoceles, and accounted for 18.8% of CSD. CSD without a mass were simple (tight filum terminale, intradural lipoma) or complex (split cord malformations, caudal regression). Our suggested classification is easy to use and to remember and takes into account clinical and MRI features; we have found it useful and reliable when making a preoperative neuroradiological diagnosis in clinical practice.

Key words Spine, dysraphism · Spinal cord, tethered · Spina bifida magnetic resonance imaging

Introduction

The congenital malformations of the spine and spinal cord seen most frequently are dysraphism and caudal spinal anomalies. Although most are diagnosed at birth or in early infancy, some are discovered in older children or even adults. MRI has facilitated both diagnosis of these disorders, and earlier and individually tailored treatment.

Knowledge of normal embryology is essential for understanding the pathogenesis and neuroradiology of these anomalies. There is still a considerable confusion as to their classification. Although most classifications are strictly based on the specific derangement of embryonic development believed to produce each malformation, embryological explanations of normal and abnormal spinal development are continuously evolving. Moreover, the MRI picture of these abnormalities is complicated, and often defies rote memorising of lists of neuroradiological features. We reviewed 986 patients referred to our Spina Bifida Centre in the past 24 years, aiming to identify the most typical neuroradiological appearances, and to correlate these features with the derangements of the complex cascade of events that characterise early embryonic development. We also intended to conceive a working classification which might prove helpful in making a diagnosis in clincal practice.

Embryology

Spinal dysraphism results from derangement in the normal embryogenetic cascade occurring during a limited period, namely between gestational weeks 2 and 6. The relevant embryogenetic steps are gastrulation (weeks 2–3), primary neurulation (weeks 3–4), and sec-

ondary neurulation and retrogressive differentiation (weeks 5–6); these will be briefly discussed [1–8].

Gastrulation

By the time of implantation in the uterine wall, which begins at the end of the 1st gestational week, changes occurring in the inner cell mass of the blastocyst produce a bilaminar disc composed of two layers, the epiblast (future ectoderm), facing the amniotic cavity, and the hypoblast (future ectoderm) facing the yolk sac. Gastrulation is the process by which the bilaminar disc is converted into a trilaminar disc with formation of an intervening third layer, the mesoblast (future mesoderm). This begins by day 14 or 15, when a strip of thickened epiblast, the so-called primitive streak, appears caudally in the midline of the dorsal surface of the embryo. The primitive streak is an area of intense mitotic activity, composed of totipotential cells, and identifies the longitudinal (craniocaudal) embryonic axis. The cranial end of the primitive streak forms Hensen's node, and shows a central depression called the primitive pit. Ectodermal cells start migrating towards the primitive streak, pass inward at the primitive pit to the interface of ectoderm and endoderm, and then migrate laterally along the interface to form the interposed mesoderm. This migration occurs along defined routes to each side of the midline, but no mesodermal cells migrate along the midline; only subsequently will these paired mesodermal anlagen join along the midline to form the notochordal process. The latter contains a central lumen, the notochordal canal, continuous with the amniotic cavity at the primitive pit. During intercalation, the canalised notochordal process fuses with the underlying endoderm; the communication of the amnion with the yolk sac forms the primitive neurenteric canal. Subsequently, during excalation, the notochord rolls up and separates from the endoderm to become the definitive notochord, while the primitive neurenteric canal becomes obliterated.

Primary neurulation

At the beginning of the 3rd gestational week, the notochord induces the overlying ectoderm to differentiate into a specialised neuroectoderm. The latter, originally flat and therefore called the neural plate, is continuous laterally with the remainder of the ectoderm. On about the 18th day, the neural plate starts invaginating along its central axis to form a neural groove, which has neural folds on each side. These folds progressively increase in size and flex to approach each other, until they eventually fuse in the midline to form the neural tube. This process is traditionally said to occur first at the level of the 4th somite (future craniocervical junction) and to proceed both cephalad and caudad like a zip. The cranial end of the neural tube (anterior neuropore) closes first (24th–25th day) at the site of the lamina terminalis, whereas the caudal end (posterior neuropore) closes later (27th–28th day), thereby terminating the process of primary neurulation. However, recent studies suggest that, rather than a continuous zip-like process, closure of the neural tube occurs at as many as five separate sites [8]. Closure sites are probably controlled by separate genes belonging to the Homeobox family, expressed during early embryogenesis. Accordingly, common neural tube defects could be predicted to occur within the domains of specific closure sites (see below). During neurulation, ectodermal cells progressively disconnecting from the lateral walls of the neural folds differentiate into the neural crests, which eventually produce both spinal and sympathetic ganglia. Immediately after neural tube closure, the superficial and neural ectoderm separate from each other in a process called disjunction. The superficial layers fuse in the midline to produce a continuous skin covering to the underlying neural tube, whereas mesenchyme migrates dorsally in the interface between skin and neural tube to form the meninges, neural arches of the vertebrae and paraspinal muscles.

Secondary neurulation and retrogressive differentiation

The location of the caudal end of the neural plate (posterior neuropore) has been the subject of enduring debate. According to the most recent theories, it is at the S3–S5 level [6]. The remaining caudal sacrococcygeal metameres of the spinal cord and the filum terminale are formed by secondary neurulation and retrogressive differentiation, starting by the end of primary neurulation and continuing until approximately the 48th gestational day.

During secondary neurulation, a secondary neural tube is formed caudad to the posterior neuropore. A *caudal cell mass* of undifferentiated, totipotential cells initially appears as a result of fusion of neural ectoderm with the lower portion of the notochord. Multiple small vacuoles then appear in the caudal cell mass and progressively coalesce to form a central canal (canalisation), which will merge with the canal formed during primary neurulation. The surrounding cells will differentiate into neurons.

The following step is retrogressive differentiation, an apoptotic process in which a combination of regression, degeneration and further differentiation occurs. The segment formed by secondary neurulation and retrogressive differentiation eventually becomes the tip of the conus medullaris and filum terminale; a focal expansion of the central canal, known as the ventriculus terminalis, is found within the lumbar enlargement during secondary neurulation, but it subsequently regresses

so that no significant dilatation is detectable on MRI in most normal individuals.

Terminology

Open and closed dysraphism

The term *"dysraphism"* (from the Greek $\delta\upsilon\sigma$ = bad and $\rho\alpha\varphi\eta$ = suture) refers to a defect of closure of the neural tube, and should therefore apply to abnormalities of primary neurulation only. However, its use has been broadened to include all congenital spinal disorders in which there is anomalous differentiation and/or incomplete closure of dorsal midline structures: skin, muscles, vertebrae, meninges and nervous tissue [5]. Because of their common embryological origin, caudal spinal anomalies are also included in this group. Spinal dysraphism is classically categorised as open (OSD) and closed (CSD) (Fig. 1). OSD is characterised by exposure of the nervous tissue and/or meninges to the environment through a congenital bony defect. Conversely, CSD is covered by skin (i.e., there is no exposed neural tissue), although cutaneous stigmata, such as a hairy naevus, capillary haemangioma, dimples, discoloured patches, dystrophy and subcutaneous masses usually betray its presence [9]. As a consequence, we regard the synonym occult spinal dysraphism as not pertinent, and strongly suggest that it be abandoned.

CSD is more numerous than OSD in our series (633 vs. 353 cases), accounting for 64.2 % of patients.

Spina bifida

The term "spina bifida" merely refers to defective fusion of posterior spinal bony elements [10] but was, and still is, widely used to refer to spinal dysraphism in general. *Spina bifida aperta* or *cystica* and *spina bifida occulta* were used to refer to OSD and CSD, respectively [11], but are no longer widely used.

Placode

This is a segment of non-neurulated embryonic neural tissue, i.e., frozen at the neural plate stage [5]. A placode is found in all OSD and in several kinds of CSD; it is exposed to air in the former, and covered by the integuments in the latter. The placode may be categorised as *terminal* and *segmental,* depending on its location along the spinal cord (Fig. 2). A terminal placode lies at the caudal end of the spinal cord, and may be *apical* or *parietal,* depending on whether it involves the apex proper or a longer segment of the cord [12]. A segmental placode may lie at any level along the spinal cord; caudad to the abnormality the cord regains normal morphology and structure.

Tethered cord

Many people believe the tethered cord is some sort of malformation. It is a clinical syndrome which may ensue as a complication of myelomeningocele repair [13, 14] or as the presentation of several forms of CSD, including spinal lipomas, the tight filum terminale [15], split cord malformations [16], and the caudal regression syndrome [17]. The conus medullaris is abnormally low (below L3 vertebral level) [11]. Symptoms and signs include motor and sensory dysfunction of the legs, muscle atrophy or hypoplasia, decreased or hyperactive reflexes, urinary incontinence, spastic gait and orthopaedic deformities such as scoliosis or foot and hip deformities [16]. The tethered cord syndrome is related to anchoring of the spinal cord or filum terminale to the surrounding tissues, either primary, in CSD, or secondary to scarring or formation of a dermoid [18] in the aftermath of myelomeningocele repair. Tethering results in stretching, distortion or kinking of arterioles, venules and capillaries as well as of nerve fibres; ensuing metabolic impairment results in functional deterioration of nerve cells in the spinal cord [16]. Further neurological deterioration may be superimposed if hydromyelia develops.

Clinical-neuroradiological classification

Much effort has been expended in the description of radiological features of spinal dysraphism. Current classifications rely heavily on the correlation of these features with a specific derangement in the normal developmental cascade [5, 7] (Table 1). However, as knowledge about normal embryology evolves, classical teaching is revised and traditional classification schemes are challenged. From a practical perspective, however, it is important to use a conceptual framework which may prove helpful to make a diagnosis, by identifying factors which critically restrict the scope of possible differentiation. These may be clinical or neuroradiological. The result of such an approach in everyday clinical practice has been a working, mixed clinical-neuroradiological classification we have found useful to orientate one to the diagnosis (Table 2). The first step in this approach is clinical: is the malformation exposed to air or is covered by intact skin? Simply, the first categorisation is into *OSD* and *CSD.*

OSD usually causes little, if any, diagnostic puzzle to the neuroradiologist. Only four varieties of OSD exist: myelomeningocele, myelocele, hemimyelomeningocele and hemimyelocele, and of these, myelomeningocele accounts for the lion's share (98.8 % of our cases).

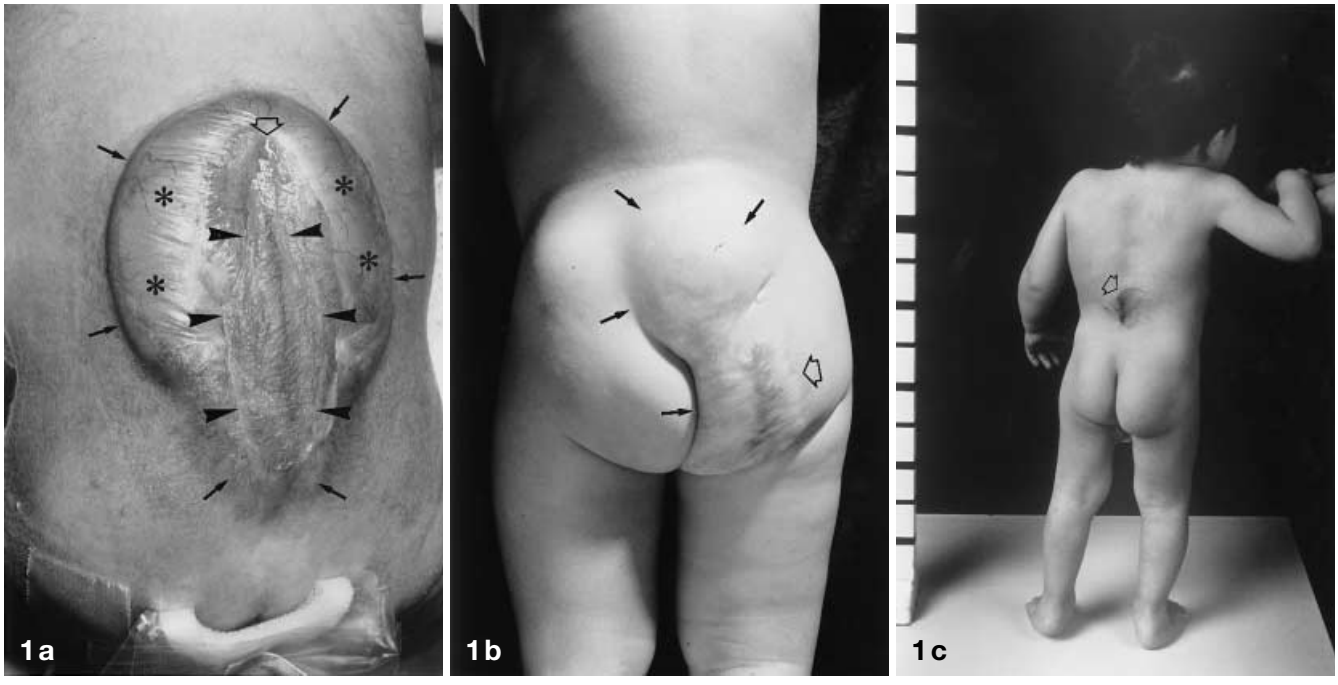

Fig. 1a–c Clinical features of open and closed spinal dysraphism. **a** Open spinal dysraphism: myelomeningocele. Low back of a 1-hour-old newborn prior to surgery. The wide placode *(arrowheads)* is directly exposed to the environment and is surrounded by partially epithelised skin (membranoepithelial zone) *(asterisks)*. More laterally, intact skin is elevated by the underlying expanded subarachnoid space *(arrows)*. Cerebrospinal fluid (CSF) dribbles out of the spinal canal at the cranial extremity of the placode *(open arrow)*. **b** Closed spinal dysraphism with a subcutaneous mass: lipomyeloschisis. Low back of a 1-year-old child. A large subcutaneous mass lies above the intergluteal crease and extends asymmetrically into the right buttock *(arrows)*. There is continuous skin covering, although the skin itself is dystrophic *(open arrow);* this is an example of why the term "occult spinal dysraphism" should be discarded, as the malformation is clearly not occult. **c** Closed spinal dysraphism without a subcutaneous mass: diastematomyelia. Back of a 2-year-old child showing a high lumbar hairy tuft *(open arrow)*. Hairy tufts may be present in several varieties of closed spinal dysraphism; however, when they lie relatively high there is reason to suspect a underlying split-cord malformation

Fig. 2a–d Myelomeningocele: different kinds of placode. **a, b** Terminal apical placode. The spinal cord crosses the meningeal outpouching and ends with the placode, which is exposed to air *(white arrow)*. Note cerebellar peg due to Chiari II malformation *(arrowhead)*. **c** Terminal parietal placode. The un-neurulated segment of the spinal cord *(arrows)* is longer than in purely apical placodes (same case as Fig. 1 a). **d** Segmental placode in a patient who had surgery for a thoracic myelomeningocele. The placode lies at T10, at the site of surgery *(arrow)*. The neurulated spinal cord caudad to the malformation regains the spinal canal and ends with a normally positioned conus medullaris

Table 1 Embryological classification of spinal dysraphism

- Anomalies of gastrulation
  - Disorders of notochord formation
    - Caudal regression syndrome
    - Segmental spinal dysgenesis
  - Disorders of notochordal integration
    - Dorsal enteric fistula
    - Neurenteric cysts
    - Split cord malformations (diastematomyelia)
    - Dermal sinus
- Anomalies of primary neurulation
  - Myelomeningocele
  - Myelocele
  - Lipoma with dural defect
    - Lipomyelomeningocele
    - Lipomyeloschisis
  - Intradural lipoma
- Combined anomalies of gastrulation and primary neurulation
  - Hemimyelocele
  - Hemimyelomeningocele
- Anomalies of secondary neurulation and retrogressive differentiation
  - Lipoma of filum terminale
  - Tight filum terminale
  - Abnormally long spinal cord
  - Persisting terminal ventricle
  - Terminal myelocystocele
- Anomalies of unknown origin
  - Cervical myelocystocele
  - Meningocele

Table 2 Cliniconeuroradiological classification of spinal dysraphism

- Open spinal dysraphism
  - Myelomeningocele
  - Myelocele
  - Hemimyelomeningocele
  - Hemimyelocele
- Closed spinal dysraphism
  - With a subcutaneous mass
    - Lumbosacral
      - Lipoma with dural defect
        - Lipomyelomeningocele
        - Lipomyeloschisis
      - Terminal myelocystocele
      - Meningocele
    - Cervical
      - Cervical myelocystocele
      - Cervical myelomeningocele
      - Meningocele
  - Without a subcutaneous mass
    - Simple dysraphic states
      - Posterior spina bifida
      - Intradural and intramedullary lipoma
      - Filum terminale lipoma
      - Tight filum terminale
      - The abnormally long spinal cord
      - Persistent terminal ventricle
    - Complex dysraphic states
      - Dorsal enteric fistula
      - Neurenteric cysts
      - Split cord malformations (diastematomyelia and diplomyelia)
      - Dermal sinus
      - Caudal regression syndrome
      - Segmental spinal dysgenesis

Usually, OSD is at the lumbar or lumbosacral level and suspected antenatally by maternal serum biochemistry and ultrasound. Clinically, *myelomeningoceles* are characterised by elevation of the neural placode by the underlying expanded subarachnoid space, whereas in *myelocele* the placode is flush with the surface of the back. This differentiation is clinical and the neuroradiologist plays little part in it. Conversely, it is the neuroradiologist's role to identify the extremely rare cases in which the myelo(meningo)cele affects one of the two hemicords of a split spinal cord. These entities, *hemimyelocele* and *hemimyelomeningocele,* are very rare and difficult to identify on a purely clinical basis and, often, even at surgery [19, 20]. More importantly, the neuroradiologist plays a critical part in the assessment of: the Chiari II malformation which, as will be detailed later on, is seen in all cases of OSD [21, 22]; associated hydrocephalus; and the complications of myelomeningocele closure (retethering by scar, dermoid, arachnoid cyst) [13, 14, 18].

CSD is much more heterogeneous than OSD and a large number of malformations belong to this wide group. Some are not clinically evident at birth, and patients may seek medical attention when complications such as the tethered cord syndrome ensue later in infancy. In general, however, clinical examination may help to restrict differential diagnosis. A critical factor is the presence of a subcutaneous mass in the back. In the vast majority of cases, this is at the lumbar or lumbosacral level. Only four malformations present with a subcutaneous mass in this location: *lipomyeloschisis, lipomyelomeningocele, meningocele* and *terminal myelocystocele.* Whereas the latter two are extremely rare, in both lipomyeloschisis and lipomyelomeningocele the mass is a subcutaneous lipoma. However, in lipomyeloschisis the lipoma gains to the spinal canal through a wide bony spina bifida, to attach to the neural placode; in other words, the placode-lipoma interface lies within the spinal canal. Conversely, in lipomyelomeningocele, ballooning of the subarachnoid spaces pushes the neural placode out of the spinal canal, so that the placode-lipoma interface lies outside the spinal canal. Simple assessment of the position of the placode-lipoma interface therefore allows confident diagnosis.

In the neck, CSD with a subcutaneous mass is represented by cervical myelomeningocele, myelocystocele and meningocele; because these entities are exceedingly rare, it is at present not clear whether they are

separate anomalies or, rather, represent variants of a single malformation.

CSD without a subcutaneous mass may also benefit from a thorough clinical assessment. The hairy patch, cutaneous angioma and skin discolouration are reliable indicators of several malformations; however, when a hairy tuft lies relatively cephalad, i.e., is midthoracic, a split cord malformation is more likely. Dorsal dimples or pinpoint ostia indicate a dermal sinus. The caudal regression syndrome may be betrayed by lower limb abnormalities or anorectal malformations, whereas newborns with segmental spinal dysgenesis show a bony protuberance along the back and have congenital paraparesis or -plegia [23]. A tethered cord syndrome may be caused by a host of malformations including the tight filum terminale, lipoma of the filum and split cord malformations. Although clinical data are critical for focussing one's attention on a specific subset of dysraphism, it is in the category of CSD without a subcutaneous mass that the neuroradiologist can be most severely challenged to attain a final diagnosis.

Open spinal dysraphism

Myelomeningocele

In myelomeningocele, a segment of the spinal cord (placode) fails to neurulate and protrudes, together with the meninges, through a bony defect in the midline of the back, thus being exposed to the environment. Because of the expansion of the underlying subarachnoid space, the surface of the placode is elevated above the skin surface, which distinguishes this anomaly from the far less common myelocele (see below). Myelomeningocele represents 98.8% of OSD in our series (349 cases); its incidence is 0.6 per 1000 live births, but is decreasing, thanks to antenatal screening procedures. Dietary supplements of folic acid to the mother prior to and during pregnancy are also protective [24].

Embryologically, myelomeningocele results from faulty primary neurulation [5, 7], probably caused by a lack of expression of carbohydrates on the surface of neurons in the developing neural tube [25]. Faulty flexion and fusion of the neural folds to form a neural tube leads to persistence of a portion of non-neurulated neural tissue, frozen at a neural plate stage, the so-called placode (Fig. 1). The external surface of the placode represents what should have become the walls of the central canal of the spinal cord, and is covered by a rich network of small, friable vessels. This raw, reddish vascular area, termed the *medullovascular zone,* shows a midline groove, probably related to the primitive neural groove, freely communicating with the central canal of the normal spinal cord above. The membrane surrounding the placode, the *membranoepithelial zone,* is composed of pia-arachnoid on the ventral surface facing the subarachnoid space, and of partially epithelised connective tissue on the dorsal surface, where the dural coating is absent. Because the cutaneous ectoderm does not separate from the neural ectoderm, it is forced to remain in a lateral position; a midline defect therefore results. As the mesenchyme cannot migrate behind the neural tube, bones, cartilage, muscles and ligaments are also forced to develop anterolateral to the neural tissue and therefore appear everted. Laterally, the placode and meninges are continuous with the subcutaneous tissue, producing spinal cord tethering. The ventral surface of the placode is formed by the would-be external surface of the spinal cord, and is therefore coated by a pia-arachnoid membrane. Nerve roots originate directly from this surface and lie approximately in the same plane, the sensory roots being the more lateral on each side of the midline. These nerve roots course obliquely through the subarachnoid space to reach the neural foramina.

The majority of myelomeningoceles are sacral or lumbosacral, and the placode is terminal, i.e., it lies at the caudal end of the spinal cord (Fig. 2). However, purely lumbar, thoracolumbar and thoracic myelomeningoceles do occur, in which the placode is segmental, and the spinal cord caudal to the malformation is normally neurulated (Fig. 2). This observation challenges the traditional concept of zip-like neurulation, in which the process of flexion and fusion proceeds bidirectionally as a sort of continuous "wave" [5]; should this "wave" be interrupted at an intermediate level (e.g., midthoracic), one would not see why it should reappear unaffected caudally. However, recent studies by Van Allen et al. [8] have suggested that the neural tube closes independently at as many as five separate sites: sacral myelomeningoceles result from failure of closure at site 5, whereas lumbar myelomeningoceles are caused by failure of closure at 1. Thoracic myelomeningoceles are rare, because they require two separate events, failure of lower closure at 1 and partial compensation by closure of 5. These concepts are intriguing, as they point to the segmental nature of the embryo. According to this theory, neural tube defects may be viewed as a single family of disorders whose difference lies in the segmental level and extent of the original damage. For instance, defects in the cranial closure sites will account for the variants of cephalocele, including the Chiari III malformation [8].

According to some workers [26], cervical myelomeningoceles form a distinct subset differing radically from classical lumbosacral myelomeningoceles, due mainly to the fact that they are covered by full-thickness skin at their base and thick squamous epithelium over the dome, and therefore belong to the category of CSD with a subcutaneous mass. However, there is still no widespread consensus as to whether these anomalies exist at all or represent a variety of myelocystocele (see below).

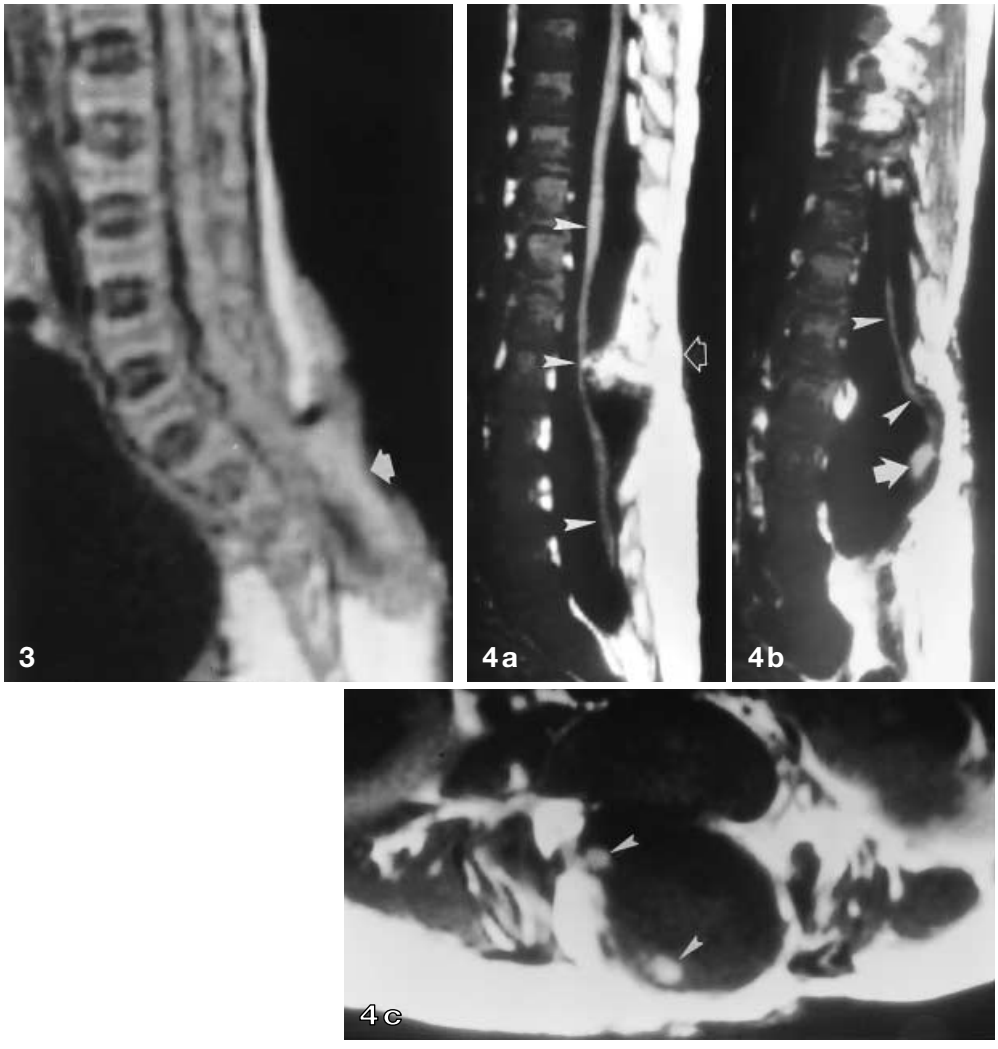

Fig. 3 Myelocele in a 1-day-old newborn. Sagittal T1-weighted image shows exposed, slightly funnel-shaped placode *(arrow)* lying flush with the skin surface. The lack of expansion of the subarachnoid space is the only difference from the much more common myelomeningocele

Fig. 4a–c Hemimyelomeningocele. **a** Slightly off-midline sagittal T1-weighted image shows one hemicord *(arrowheads),* which is thin at the level of a repaired open spinal dysraphism *(open arrow)* and extends inferiorly to S1. **b** Parasagittal T1-weighted image shows a second hemicord *(arrowheads)* projecting into the meningeal outpouching. There is a small lipoma inferiorly *(arrow).* **c** Axial T1-weighted image shows diastematomyelia without septum, with widely splayed hemicords *(arrowheads).* Courtesy Dr. M. Castillo, Chapel Hill, NC, USA)

Because of the risk of ulceration and ensuing infection, myelomeningocele and myelocele are neurosurgical emergencies; therefore, affected newborns are rarely imaged prior to surgery. It is, however, our policy to perform preoperative MRI when possible, to obtain an anatomic characterisation of the components of the malformation, i. e., the relationship between the placode and nerve roots; presurgical assessment of the malformation: hydromyelia, hydrobulbia, Chiari II malformation and hydrocephalus [22]; and to identify those rare cases with associated cord splitting (hemimyelomeningoceles and hemimyeloceles).

Myelocele

Myelocele (myeloschisis) differs from the much more common myelomeningocele in that the subarachnoid space ventral to the placode is not expanded; as a consequence, the placode lies flush with the cutaneous surface or is funnel-shaped (Fig. 3) [5]. Embryologically, the same principles apply as for myelomeningoceles; indeed, the myelocele is equivalent to the myelomeningocele, the only difference being the absence of expansion of the underlying subarachnoid space. This is an extremely rare malformation, representing only 1.2 % of OSD in our series (four cases).

Hemimyelo(meningo)cele

Myelomeningoceles and myeloceles are associated with split-cord malformations (SCM) (diastematomyelia) in 8–45 % of cases [19, 27]. However, if the cord is split at a different level from the placode, the malformation is merely an association of SCM and OSD. Only when one hemicord fails to neurulate is the terms hemimyelocele or hemimyelomeningocele (when there is meningeal

protrusion) (Fig. 4) appropriate. If this restrictive definition is accepted, these anomalies become extremely rare; we did not see a single case in 24 years. Neurological impairment is reported to be markedly asymmetric [20].

Embryologically, these malformations are related to faulty gastrulation (see below, split cord malformations) with superimposed failure of primary neurulation of one or, in exceptional cases, both hemicord(s) [3].

The Chiari II malformation

OSD is always accompanied by a Chiari II malformation, a complex congenital anomaly of the hindbrain characterised by a posterior cranial fossa which is smaller than normal, with caudal displacement of the vermis, brain stem and fourth ventricle. The association is constant.

McLone and Knepper [28] produced a theory to explain this constant association. Because the neural tube remains non-neurulated, during gestation CSF leaks through the spinal defect into the amniotic sac, resulting in chronic CSF hypotension within the developing neural tube. As a result, the rhombencephalic vesicle (developing fourth ventricle) fails to expand, and fails to induce the perineural mesenchyme of the posterior cranial fossa. Therefore, both cerebellum and brain stem are eventually forced to develop within a small posterior cranial fossa, and consequently herniate through both the tentorial groove and the foramen magnum [29]. CSF hypotension in the supratentorial brain may also impair neuronal migration and bony development, producing various associated anomalies of the nervous tissue and its osteomeningeal coating.

The Chiari II malformation is more than an associated feature with OSD; it should be regarded as part of the malformation sequence [22]. However, the severity of the hindbrain malformation is variable, so that patients with a posterior cranial fossa of nearly normal size are found [21, 22]; subtle, minimal features of Chiari II malformation may therefore be seen in all newborns with OSD.

The Chiari II malformation is absent in all types of CSD with the only possible exception of myelocystoceles, in which venting of CSF in a large subcutaneous meningocele may result in CSF hypotension within the developing neural tube (T. P. Naidich, personal communication).

Closed spinal dysraphism

With a subcutaneous mass

These abnormalities are characterised by a skin-covered mass which indicates the underlying malformation; the overlying skin is frequently abnormal. Because there is a strong tendency for certain malformations to occur only at given segmental levels, different entities have to be considered, depending on the location of the mass. Most often, the mass is at the lumbosacral level right above the natal cleft, when conditions are found: the quite common lipoma with a dural defect (lipomyeloschisis and lipomyelomeningocele), and the distincly uncommon terminal myelocystocele and meningocele; the main differential diagnosis is from sacrococcygeal teratomas and overgrowing fatty tissue in caudal regression, which, however, is more caudal, at or below the natal cleft. Conversely, if the mass is cervical three anomalies should be considered: cervical myelomeningocele, myelocystocele and meningocele; the main differential diagnosis is from occipitocervical cephalocele and subcutaneous masses such as lymphangioma.

CSD with a subcutaneous mass represents 18.8 % of CSD in our series (119 cases), lipomas with a dural defect accounting for 87.4 % of these (104 cases). We did not encounter a single case of cervical CSD with a mass, in keeping with the extreme rarity of reported cases [26].

Lipomas with a dural defect: lipomyeloschisis and lipomyelomeningocele

Together, these anomalies accounted for 75.9 % of spinal lipomas and 16.4 % of CSD in our series; lipomyeloschisis was more than twice as common as lipomyelomeningocele (74 vs. 30 cases). In both anomalies, the intraspinal lipoma is but a portion of a larger subcutaneous lipoma, extending into the spinal canal through a wide posterior spina bifida and tethering the spinal cord. A midline subcutaneous mass right above the natal cleft and extending asymmetrically into one buttock is the rule (Fig. 1) [30]. Although the mass is evident at birth, early signs of neurological disturbance are seldom present. However, these are generally manifest by 6 months of age, with weakness and poor development of muscles of both legs, gait disturbance, urinary incontinence and sensory changes.

Histologically, the mass is composed of clusters of mature adipocytes separated by collagenous bands in 23 % of cases, whereas in the remainder a mixture of tissues of ectodermal, mesodermal or endodermal origin is present; spinal lipomas should therefore be considered as simple or complex teratomas [31]. Congenital intraspinal lipomas are anatomically stable lesions [31], but growth of the subcutaneous and intraspinal components may occur as part of the normal increase in adipose tissue throughout childhood [32], as well as in conditions such as obesity or pregnancy.

Embryologically, spinal lipomas are abnormalities of primary neurulation resulting from premature disjunc-

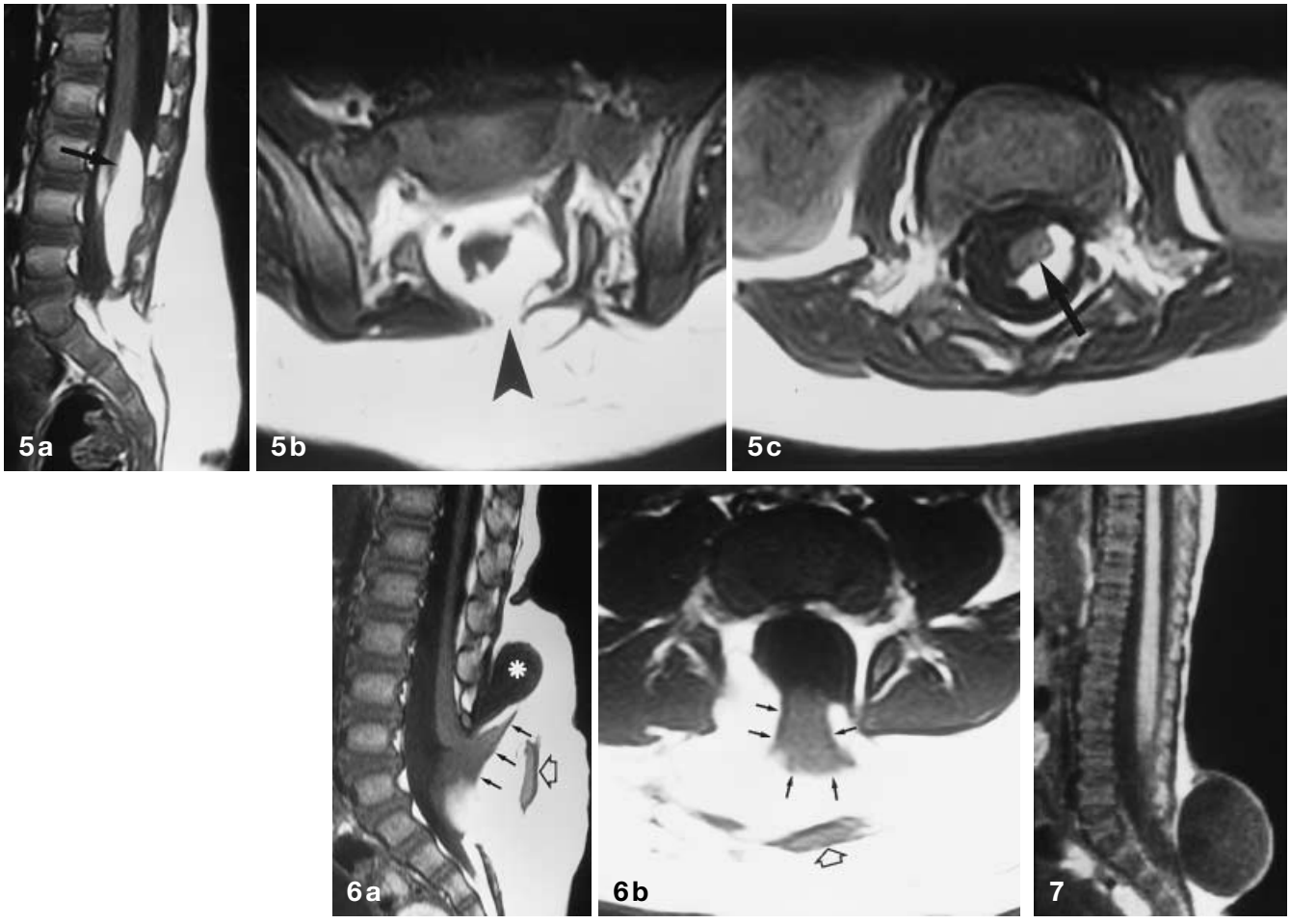

Fig. 5a–c Lipomyeloschisis. **a** Sagittal T1-weighted image shows large subcutaneous lipoma with fatty tissue creeping through a posterior spina bifida to connect with the placode. The placode-lipoma interface lies within the spinal canal *(arrow)*. **b,c** Axial T1-weighted images demonstrate that the subcutaneous lipoma is continuous with the intraspinal lipoma through a posterior spina bifida *(arrowhead)*. The placode-lipoma interface is asymmetrical and lies along the left side of the placode *(arrow)*

Fig. 6a, b Lipomyelomeningocele. **a** Sagittal T1-weighted image shows segmental placode connecting with a subcutaneous lipoma *(black arrows)* along the inferior wall of the meningeal sac *(asterisk)*. Surgically proven dysraphic hamartoma histologically composed of bone lies within the lipoma *(open arrow)*. **b** Axial T1-weighted image shows placode-lipoma interface largely outside the anatomical boundaries of the spinal canal *(black arrows)*. The dysraphic hamartoma *(open arrow)* is clearly visible

Fig. 7 Meningocele. Sagittal T1-weighted image shows a large sacral CSF-filled mass. The overlying skin is continuous, albeit markedly thinned. The conus medullaris is low

tion of cutaneous ectoderm from the neuroectoderm [5, 30]. As a consequence, mesenchyme can gain access to the interior of the neural tube, and is induced by the dorsal surface of the closing neural tube (the future ependymal lining of the central canal) to form fat, which prevents neurulation to proceed. The lateral extent of the fatty tissue is limited by the neural ridge, because the ventral surface of the neural plate (the future exterior of the neural tube) induces the mesenchyme to form meninges; therefore, the junction between fat and meninges lies exactly at the neural ridge, which divides the dorsal and ventral surfaces of the neural folds so that, strictly speaking, the lipoma is extradural [5, 30]. The lipoma then extends posteriorly through the meningeal and bony defect and into the subcutaneous tissues. Depending on its size, and the degree of expansion of the subarachnoid space, the connection between the lipoma and the spinal cord (the placode-lipoma interface) will lie within, at the edge of, or outside the spinal canal; characteristically, it is within or at the edge of the spinal canal in lipomyeloschisis (synonym: lipomyelocele), and outside it (within a meningocele) in the less common lipomyelomeningocele.

In lipomyeloschisis, both the bony defect and the subcutaneous fat extending into the spinal canal and attaching to the cord are clearly demonstrated by MRI (Fig. 5). The placode is terminal (apical or parietal), and may be asymmetrical if the premature disjunction has involved only one edge of the neural plate. The placode-lipoma interface may extend over several vertebral levels.

Lipomyelomeningoceles may produce a constellation of MRI features (Fig. 6). Unlike in lipomyeloschisis, the placode is frequently segmental; it may be deformed, stretched and rotated asymmetrically towards the lipoma on one side, whereas the meninges herniate on the opposite side. Spinal roots emerging from the latter surface are generally longer, whereas those lying on the side of the lipoma emerge nearer to the sheaths and neural foramina; they are shorter and tether the spinal cord [5]. The segment of spinal cord located below the placode is normal and lies within the spinal canal. The herniated segment may be anchored to the surface of the malformation by fibrous bands.

In both lipomyeloschisis and lipomyelomeningocele, cartilaginous, bony, fibrous, muscular, vascular or aberrant neuroglial structures may be found within the lipoma, forming *dysraphic hamartomas* (Fig. 6). The lipoma may envelope the cord to a varying extent or invade the extradural space, resulting in a *lipomatous dura mater.* Hydromyelia is present in up to 25 % of cases.

Meningocele

The classical *posterior meningocele* is characterised by herniation of a CSF-filled sac lined by dura mater and arachnoid through a posterior spina bifida (Fig. 7). It is commonly lumbar or sacral, but thoracic and even cervical meningoceles are found; the latter enter into the differential diagnosis of cervical myelocystoceles and myelomeningoceles. Spinal meningoceles are less common than usually believed: we found only 15 cases (2.4 % of all CSD). Their embryogenetic origin is unknown; it may be hypothesised that they result from ballooning of the meninges through a posterior spina bifida due to the relentless effect of CSF pulsations in the subarachnoid space.

Although both nerve roots and, more rarely, a hypertrophic filum terminale may course within the meningocele, by definition, no part of the spinal cord is within the sac, and the spinal cord itself is completely normal structurally, although it is usually tethered to the neck of a sacral meningocele [33].

Anterior meningoceles are almost always presacral and consistently found in the caudal regression syndrome (Fig. 20) [34]; they do not belong to the group of CSD with a subcutaneous mass. The same applies to the much rarer *intrasacral meningocele,* which is, by definition, an intrasacral arachnoid outpouching through a dural defect (Fig. 8) [35, 36].

Terminal myelocystocele

This is an extremely rare CSD, and we did not encounter a single case. The subcutaneous mass is in the sacrococcygeal area and contains an ependyma-lined cyst which represents a wide dilatation of the terminal ventricle *(syringocele),* which bulges through a posterior spina bifida (Fig. 9) [37–39]. The distension of the arachnoid lining of the distal spinal cord also causes herniation of the meninges, producing a meningocele. On the outer surface of the cord, both pia and arachnoid are continuous with the meningocele, while the inner surface of the syringocele is lined by ependyma; fatty and fibrous tissue and skin attach directly to the ependyma. The syringocele lies caudal to the meningocele in all cases.

The embryological origin of the terminal myelocystocele is not known. Current theories postulate a disturbance of CSF dynamics within the early neural tube of unknown cause [5], but likely to be related to abnormal retrogressive differentiation [37–39]. This anomaly probably results from the inability of CSF to exit from the early neural tube, causing the terminal ventricle to balloon into a cyst which disrupts the overlying mesenchyme. The terminal myelocystocele could then be viewed as a severe, disruptive variety of the simple persisting terminal ventricle. A Chiari II malformation may be associated.

Prognosis is mainly related to other anomalies, since children with this condition are usually neurologically intact at presentation [37]. Associated abnormalities usually belong to the OEIS constellation (omphalocele, extrophy of the cloaca, imperforate anus, spinal anomalies) [40, 41].

Cervical myelocystocele

Cervical myelocystoceles differ morphologically from terminal myelocystoceles in that only a stretched part of the dorsal wall of the hydromyelic cavity protrudes into the meningocele. However, this rarer malformation also retains an epithelial lining [5, 42]. The embryological origin is difficult to identify; in accordance with the suggested origin of terminal myelocystoceles, cervical myelomeningoceles could be viewed as the result of defective CSF dynamics during the early stages of neural tube development. The medial walls of the primitive central canal of the neural tube ("neurocele") normally appose and occlude the neurocele transiently during primary neurulation [5]. Failure to recanalise the neurocele could cause it to dilate segmentally, disrupt the overlying mesenchyme and balloon out in a cyst covered by skin.

On MRI, hydromyelia is reported to be critical to rule out cervical myelomeningoceles [26]. We saw no case of cervical myelocystocele; however, we saw a pa-

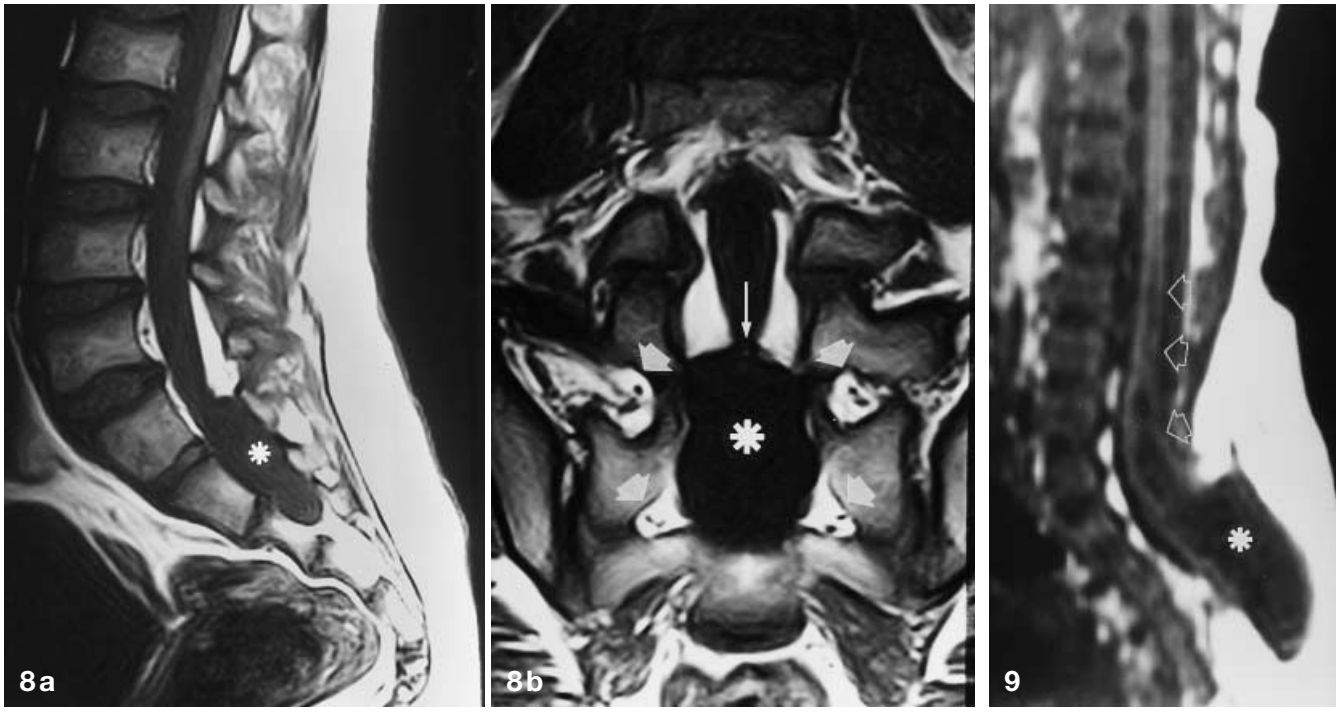

Fig. 8a, b Intrasacral meningocele. **a, b** Sagittal and coronal T1-weighted images show a cystic mass *(asterisk)* within the expanded sacral canal, connected to the dural sac through a small orifice *(thin arrow)*. The mass is isointense with CSF. The sacral foramina *(thick arrows)* are spared, which excludes a perineural cyst

Fig. 9 Terminal myelocystocele. Sagittal T1-weighted image shows a large subcutaneous syringocele *(asterisk)*, continuous with hydromyelia *(empty arrows)* through a wide spina bifida. (Courtesy Dr P. D. Barnes, Boston, MA, USA)

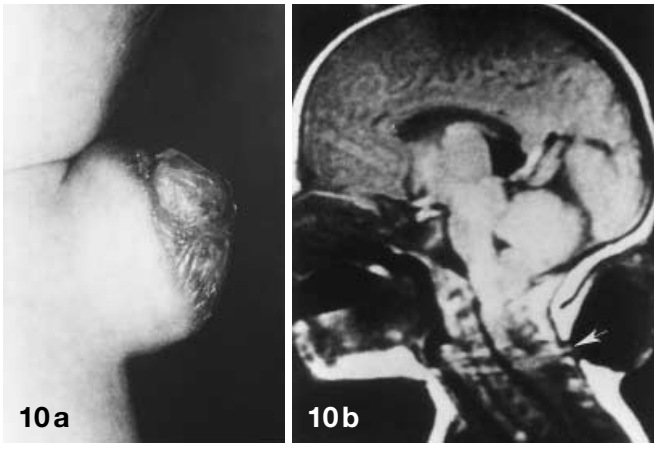

Fig. 10a, b Cervical myelomeningocele. **a** The external features are shown. The base of the sac is covered by full-thickness skin, the dome by thick, violaceous, squamous epithelium. **b** Sagittal T1-weighted image suggests a tissue nodule at the base of the sac *(arrow)*. Ectopic cerebellar tissue descends to C2-3, but is not included in the myelomeningocele. (Courtesy Dr D. Pang, Sacramento, CA, USA)

tient, previously operated for a thoracic myelocystocele, who harbored a Chiari II malformation.

Cervical myelomeningocele

Cervical myelomeningoceles are extremely rare and strikingly different from the much more common lumbosacral myelomeningocele. According to the literature, they account for 3.7 % of patients with OSD [26], but we did not encounter a single case.

According to Pang and Dias [26], cervical myelomeningoceles consist of a fibroneurovascular stalk containing neurons, glia and peripheral nerves, emanating from a limited dorsal myeloschisis and penetrating through a narrow dorsal dural opening to fan out into the lining of a meningeal sac (Fig. 10); an underlying split cord malformation is frequent. A Chiari II malformation was present in 44 % of the series of Pang and Dias [26], who speculated that the limited extent of the myeloschisis makes it unlikely that enough CSF leakage occurs to start the cascade of events leading to a Chiari II [26].

There is no widespread consensus as to whether cervical myelomeningoceles are a true, separate entity. Some workers [43, 44] found them to differ from the typical lumbosacral myelomeningocele in that neural tissue is not exposed, and questioned whether they could in fact represent limited dorsal myelocystoceles; because the spinal cord is within the spinal canal it is difficult to call these lesions myelomeningoceles. Moreover,

if one accepts the definition of Pang and Dias [26], a true "meningocele" would be unlikely, as meningoceles often contain some elements of neural tissue, such as aberrant nerve roots.

The paucity of reported cases of cervical dysraphic lesions makes it difficult to categorise them properly in both clinical and neuroradiological terms.

Without a subcutaneous mass

Simple dysraphic states

This subset of abnormalities is embryologically heterogeneous, as it includes defects of both primary and secondary neurulation. However, these may be grouped from a clinical viewpoint, as they represent the most common abnormalities in children without significant low-back cutaneous stigmata who present with symptoms and signs of cord tethering [15, 16, 45, 46].

Posterior spina bifida. The simplest variety of CSD is represented by a simple defect of fusion of the posterior neural arch of a vertebra, usually L5 or S1. It may be isolated, as an incidental finding of no clinical significance. In children with signs of cord tethering, it should suggest some other CSD. However, the normal laminae at L5 level may remain unfused until 5–6 years of age [5]. Isolated posterior spina bifida was found in 140 patients in our series [22.1 % of CSD).

Intradural and intramedullary lipoma. A lipoma is a monophyllic mass originating from the mesoderm. Embryologically, lipomas result from early disjunction between neuroectoderm and ectoderm; the surrounding mesenchyme creeps between and adheres to the primitive ependyma, which induces it to transform into fat [5].

Lipomas are more or less completely capsulated and lobulated by fibrous bundles. Intradural lipomas are commonly at the lumbosacral level, but may be found anywhere in the spinal canal; they may be multifocal or huge. They are generally subpial. In rare instances, they are completely intramedullary or produce diffuse medullary lipomatosis. Intradural lipomas accounted for 24.1 % of spinal lipomas in our series. On MRI (Fig. 11), they are isotintense with subcutaneous fat in all sequences, i. e., they give high signal on T1- and conventional spin-echo T2-weighted images, and high signal on fast spin-echo T2-weighted images.

Filum terminale lipoma. This is an elementary anomaly of secondary neurulation characterised by fibrolipomatous thickening of the filum terminale. In a small percentage of cases, it may be detected in adulthood, and may be considered an anatomical variant if part of a tethered cord syndrome. Both not the intra- and the extradural portions of the filum terminale may be involved. This anomaly is probably due to residual totipotential cells of the caudal cell mass differentiating into fatty tissue [47]. MRI shows fat within a thickened filum terminale (Fig. 12). Because the filum is frequently slightly off the midline, axial T1-weighted images are most useful for diagnosis.

Tight filum terminale. This is a simple, albeit rare, disorder of retrogressive differentiation. We saw 57 cases of tight filum terminale and filum terminale lipoma, representing 9 % of CSD. The tight filum terminale is characterised by a short, hypertrophic filum terminale producing tethering and impaired ascent of the conus medullaris (Fig. 13). By definition, no other dysraphic state is present, with the possible exception of a dermal sinus. The conus medullaris is frequently low. Embryologically, a tight filum is related to abnormal retrogressive differentiation of the secondary neural tube, producing a thicker than normal filum. This anomaly may be difficult to diagnose, although the association of clinical and neurological features may be suggestive; axial MRI may be definitive: the abnormal filum terminale must exceed 2 mm in diameter [48] and no fatty tissue must be present, otherwise the abnormality is best defined as a lipoma or fibrolipoma (see above). Posterior spina bifida, scoliosis and kyphoscoliosis are present in a high percentage of cases.

The abnormally long spinal cord. This abnormality may be considered a variant of the previous one, and is characterised by the absence of a normally tapered conus medullaris. The spinal cord does not show significant changes in calibre down to the sacrum, where it connects with the lower end of the thecal sac. To the best of our knowledge it has never been described on imaging, and might be embryologically related to a complete retrogressive differentiation of the secondary neural tube. It may occur alone or in association with other features of CSD such as intradural lipoma or lipomyelomeningocele.

Persistent terminal ventricle. The "fifth ventricle" of the older literature [49] is a small ependyma-lined cavity in the conus medullaris which is always identifiable on postmortem examination, but must achieve a certain size to become visible on MRI (Fig. 14) [50]. Embryologically, it represents incomplete regression of the terminal ventricle of the secondary neurulation, with preservation of its continuity with the central canal of the rostral spinal cord. The latter point is critical because, according to present theories [5], failure of regression of the terminal ventricle without a patent connection to the central canal above may produce a terminal myelocystocele, a much more severe and disruptive

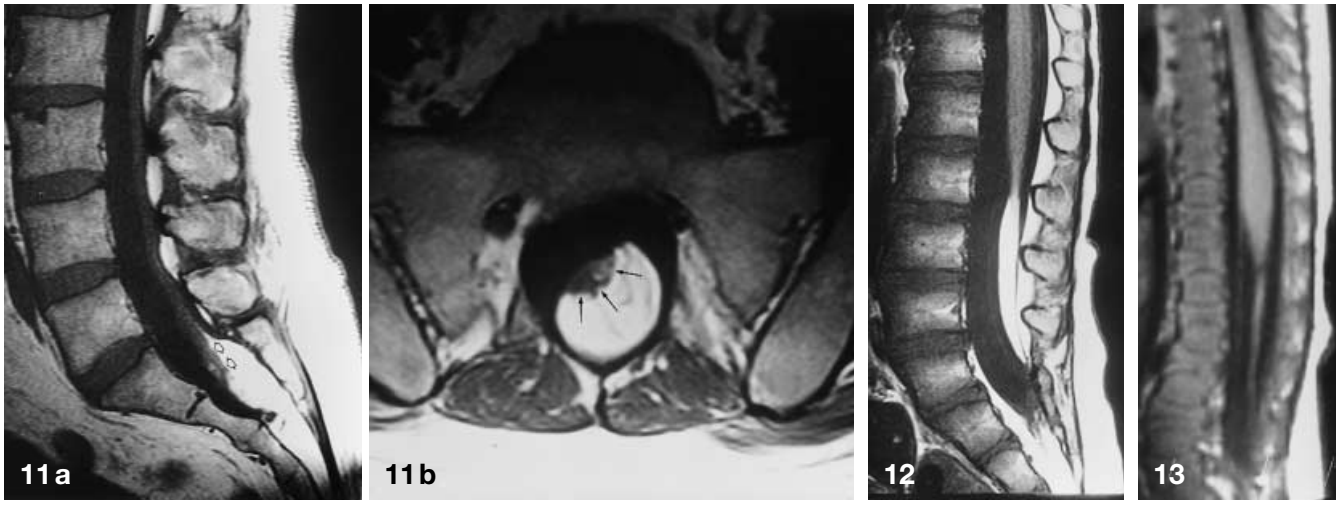

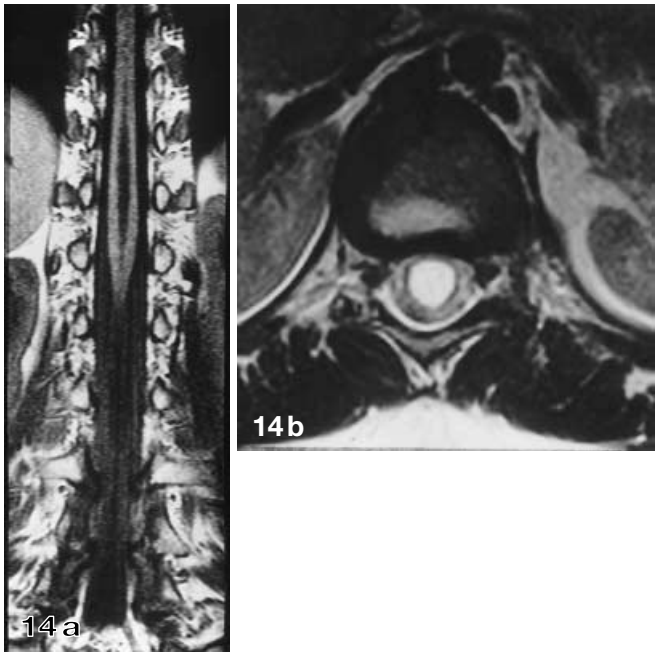

Fig. 11a, b Intradural lipoma. **a** Sagittal T1-weighted image shows the spinal cord tethered to the anterior surface of a sacral lipoma *(open arrows)*. The spinal canal is slightly wide, with a scalloped posterior surface to the S2 vertebral body. **b** Axial T1-weighted image shows the placode-lipoma interface *(arrows)*. The placode is slightly rotated to the left. The lipoma is intradural and clearly separated from the subcutaneous fat

Fig. 12 Lipoma of filum terminale. Sagittal T1-weighted image shows that the filum is largely replaced by fat. The spinal cord is tethered and low

Fig. 13 Tight filum terminale. Sagittal T1-weighted image shows thickened filum terminale with tethered, low conus medullaris

Fig. 14a, b Persistent terminal ventricle. **a** Coronal T1-weighted image shows an intramedullary cavity in the conus medullaris, at the anatomical site of the terminal ventricle. The anomaly is indistinguishable from diastematomyelia in this plane. **b** Axial T2-weighted image shows no diastematomyelia

abnormality. In itself, the persisting terminal ventricle is asymptomatic; however, cases have been reported in which huge cystic dilatation was seen in patients with low-back pain, sciatica and bladder disturbance, possibly secondary to thinning of the spinal cord tissue by the cyst [51]. It is not clear whether these "terminal ventricle cysts" are developmental variants or result from pathological obstruction of the terminal ventricle [50]. The differentiation from hydromyelia is based on its being found immediately above the filum terminale. A intramedullary tumour is unlikely in the absence of contrast enhancement; the size of the "cyst" remains unchanged on follow-up.

Complex dysraphic states

Because gastrulation is characterised by the development of the notochord, spinal dysraphism originating in this period will characteristically shows a complex picture, in which not only the spinal cord, but also other organs deriving from or induced by the notochord are severely abnormal. Disorders of gastrulation are therefore also sometimes called complex dysraphic states [3]. In the vast majority of cases, the abnormalities are covered by skin and no tell-tale subcutaneous mass is present. The sole exception is hemimyelocele and hemimyelomeningocele, two exceedingly rare abnormalities described in the open spinal dysraphism section.

Failures of notochordal development may essentially be traced back to two subsets of derangement: failures of midline notochordal integration, resulting in longitudinal splitting and failures of notochordal formation, resulting in the absence of a given notochordal segment.

Disorders of midline notochordal integration. Midline integration is the process by which the two paired notochordal anlagen fuse in the midline to form a single notochordal process. If these notochordal precursors fail to integrate, they remain separate and develop independently over a variable segment, and the intervening space will be occupied by totipotential primitive-streak cells [3]. The cause of notochordal splitting is the source of continuing debate, and several possible explanations have been put forward, such as endo-ectodermal adhesion within the primitive streak [52], initial teratogenic or spontaneous mutation of the developing notochord [53] and persistence or only partial obliteration of the neurenteric canal [19]. Recently, Dias and Walker [3] demonstrated that separation of Hensen's node into two independent halves during gastrulation results in a duplicated notochord and neuraxis. Regardless of the underlying cause, the type of malformation will depend on the level and extent of the defect and on the success of subsequent reparative efforts [3, 52]. The split notochord syndrome includes several apparently quite different entities such as the dorsal enteric fistula, neurenteric cysts, diastematomyelia, dermal sinuses and even intestinal duplication. The differences between these entities result from the different developmental fate of the intervening primitive-streak tissue towards endo-, meso- or ectoderm; however, they all share some degree of vertebral abnormality (block vertebrae, butterfly vertebrae, hemivertebrae), pointing to the original notochordal abnormality.

Dorsal enteric fistula

This is an exceedingly rare condition, representing the most severe complex dysraphic state, and consisting of a cleft connecting the bowel with the dorsal skin surface through the prevertebral soft tissues, vertebral bodies, spinal canal and its contents, neural arch and subcutaneous tissues. The involved segment of both the vertebral column and spinal cord is split, to form two columns surrounding the cleft. We encountered no case of complete dorsal enteric fistula, and few cases are in the recent literature. In the case reported by Hoffman et al. [54], there was bifurcation of the spine and spinal cord at the lumbar level with continuation to a conus medullaris bilaterally. Castillo et al. [55] reported a case with duplication of L5 and the sacrum and duplication of the spinal cord in a child with prior surgery to a cyst in the lower back whose nature could not be ascertained.

Embryologically, dorsal enteric fistula is due to failure of notochordal integration with full-thickness persistence of the neurenteric canal. There is reportedly a strong association with malformations of viscera such as renal dysplasia, diaphragmatic hernia, pulmonary hypoplasia, cardiac anomalies [3] and the OEIS complex [54].

Neurenteric cysts

These are found within the spinal canal and are lined by mucin-secreting, cuboidal or columnar epithelium resembling the gastrointestinal tract [3]. Their contents are variable, and their chemical composition may be similar to CSF. The typical location is intradural in the thoracic spine, anterior to the spinal cord [56, 57]; however, neurenteric cysts may also be found in the cervical (Fig. 15) or lumbar spine, and even in the posterior cranial fossa, and they are posterior to or even within the spinal cord in a minority of cases. Vertebral abnormalities are commonly present.

Embryologically, neurenteric cysts may be due to endodermal differentiation of primitive-streak remnants, possibly related to incomplete regression of the neurenteric canal. As such, they are but the intraspinal counterpart of gut duplications, in which the abnormality develops in close proximity to the gastrointestinal tract rather than the spinal cord. Differential diagnosis between neurenteric cysts and gut duplication is just a matter of site [58].

We saw two cases of this rare abnormality. The largest recent series is that of Gao et al. [57], who reported on 31 surgically proven neurenteric cysts. Although the MRI appearances were variable, reflecting their contents, most were isointense or gave slightly higher signal than CSF on T1- and high signal on T2-weighted images. Absence of contrast enhancement was the rule; however, we saw a neurenteric cyst which did enhance.

Split-cord malformations (SCM)

These entities are classically defined as diastematomyelia (from the Greek $\delta\iota\alpha\sigma\tau\eta\mu\alpha$ = cleft) and diplomyelia ($\delta\iota\pi\lambda o\upsilon\zeta$ = double). Although from a strict etymological perspective diastematomyelia means spinal cord splitting and diplomyelia cord duplication, there has been no widespread consensus on use of these terms in the radiological literature, mainly due to the inherent difficulty in assessing true cord duplication preoperatively. We saw 24 cases, accounting for 3.8 % of CSD.

Embryologically, the two paramedian notochordal anlagen are prevented from integrating in the midline, probably by a persistent anomalous communication between the yolk and amniotic cavities (neurenteric ca-

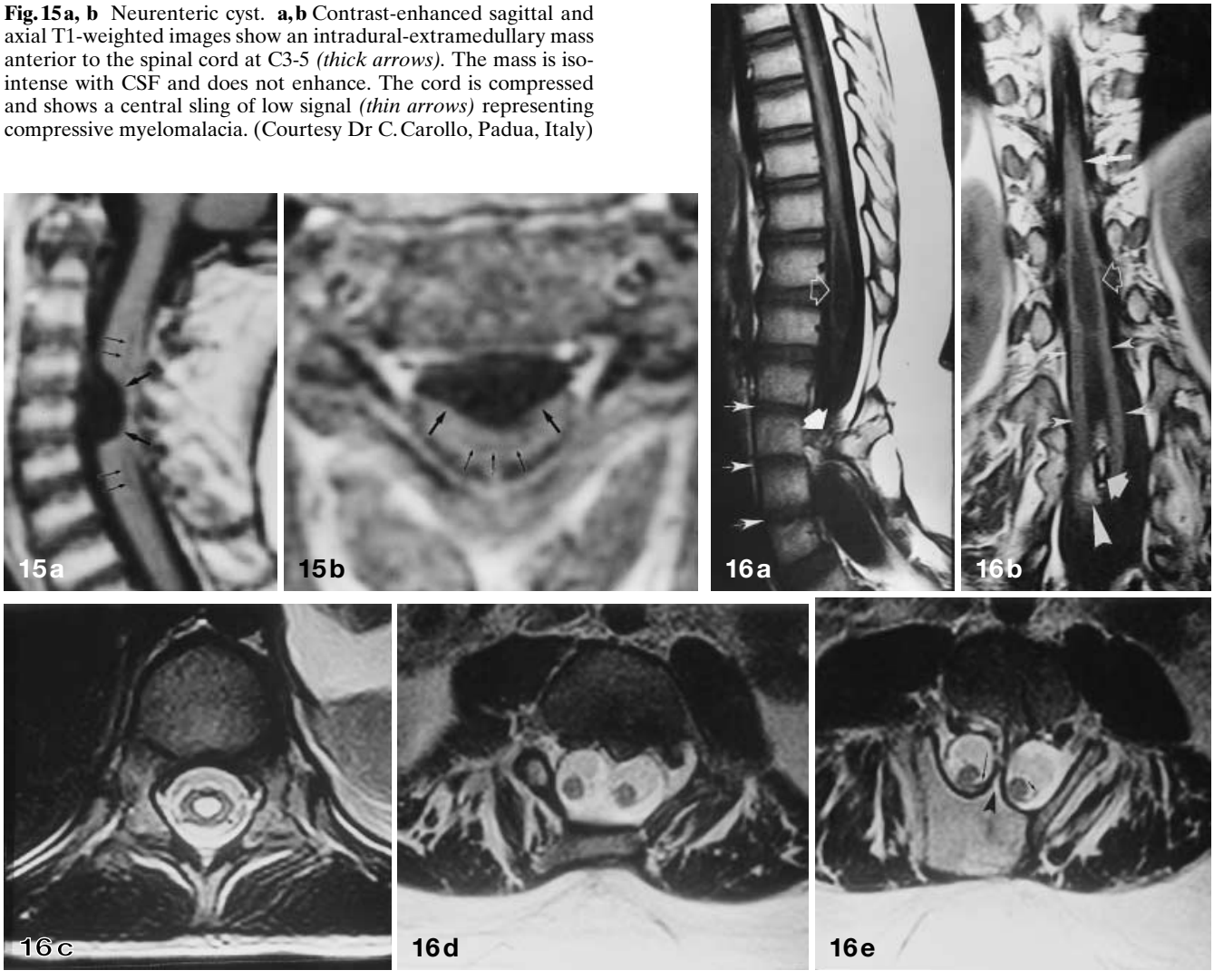

Fig. 15a, b Neurenteric cyst. **a, b** Contrast-enhanced sagittal and axial T1-weighted images show an intradural-extramedullary mass anterior to the spinal cord at C3-5 *(thick arrows)*. The mass is isointense with CSF and does not enhance. The cord is compressed and shows a central sling of low signal *(thin arrows)* representing compressive myelomalacia. (Courtesy Dr C. Carollo, Padua, Italy)

Fig. 16a–e Type I split cord malformation (diastematomyelia with septum). **a** Sagittal T1-weighted image shows bony spur *(thick arrow)* projecting into the spinal canal. There is thoracolumbar hydromyelia *(open arrow)*. A vertebral segmentation defect is revealed by rudimentary intervertebral discs at L1–4 *(thin arrows)*. **b** Coronal T1-weighted image shows the midline bony spur to lie at the caudal end of the split in the cord splitting and to contain high-signal bone marrow *(thick arrow)*. The craniocaudal malformation sequence includes a normal spinal cord *(long arrow)*, hydromyelia *(open arrow)*, and diastematomyelia *(thin arrows)*. Note lipoma adjacent to right hemicord *(arrowhead)*. **c–e** Axial T2-weighted images show the malformation sequence from cephalad to caudad: **c** hydromyelia, **d** diastematomyelia within single dural sac and **e** diastematomyelia with dual dural sacs and intervening bony spur *(arrowhead)*. Axial views also show that the right hemicord has one paramedian set of nerve roots connected to the bony spur (*long arrow* **e**), while a posterior root is clearly seen as it merges with the left hemicord (*short arrow* **e**)

nal), around which the intervening primitive streak condenses to form the so-called endomesenchymal tract [19]. Failure of midline notochordal integration produces two separate, variably elongated notochordal columns, each of which induces a separate neural plate. The resulting malformation depends on the developmental fate of the endomesenchymal tract: if the primitive-streak tissue further develops towards bone and cartilage, the two hemicords will be eventually contained in two separate dural sacs, separated by a osteocartilagineous spur; conversely, if the endomesenchymal tract totally regresses or leaves a thin fibrous septum, the two hemicords will lie within a single dural tube.

In 1992, Pang et al. [19] suggested that terms such as diastematomyelia and diplomyelia be abandoned, to make way for a new classification of SCM in two types, based on the state of the dural tube and the nature of the median septum.

- Type I SCM (diastematomyelia with septum). This was the less common of the two varieties in our series (25 % of cases). Clinically, the patients usually present with scoliosis and a tethered cord syndrome. Cutaneous birthmarks such as haemangioma, dyschromic patches and hairy tufts often betray the underlying malformation; a hairy tuft high along the back is a quite reliable clinical marker of type I SCM. Vertebral anomalies are the rule, and include block or butterfly vertebrae, hemivertebrae and posterior spina bifida. The radiological hallmark [19, 59] is the osseous or osteocartilagineous midline septum with resulting double dural tubes, each containing a hemicord (Fig. 16). The spur may be complete or incomplete and course sagittal or obliquely; in some cases it divides the spinal canal unequally, and the two hemicords will be asymmetrical. The cleft is generally thoracic or lumbar and always lies at the caudal end of the split; the two hemicords usually surround the spur tightly, before fusing with each other to form a normal spinal cord below, whereas rostrally the split is much more elongated. The cleft is terminal in some cases, and two hemicones and hemifilum (generally hypertrophic and tethered) are formed. Hydromyelia is a common finding, and may involve the normal cord both above and below the split as well as one or both the hemicords [60]. Failure of neurulation of one hemicord produces a hemimyelocele or hemimyelomeningocele; these are extremely rare, and we saw no such case (see Open spinal dysraphism).
- Type II SCM (diastematomyelia without septum). The radiological hallmark is a single dural sac containing both hemicords (Fig. 17) [19, 61]. No osteocartilagineous spur is found, although a fibrous septum is usually present at surgery; in these cases, signs of cord tethering may appear, and indeed the assumption that type II SCM does not produce a tethered cord syndrome is incorrect [20]. The fibrous septum may be very thin, and is usually best appreciated on coronal or axial T2-weighted images. In some cases, the cleft is partial and the split incomplete; these are the mildest forms of diastematomyelia [12]. Hydromyelia may be present, with the same features as in type I. Vertebral anomalies are usually milder than in type I, and consist of butterfly vertebrae in most cases. Posterior spina bifida is often present.

As stated previously, whether each neural plate is complete or rather a "hemineural" plate has been the source of much debate, as this distinction implies spinal cord duplication or splitting. It has traditionally been believed that the examination of paramedian nerve roots may clarify this problem, as only truly duplicated cords would possess double sets of dorsal and ventral roots, whereas split hemicords would only have one [59]. However, Pang et al. [19] have shown that both types of SCM may show paramedian nerve roots, depending on whether neural crest cells (which produce the roots) are trapped within the endomesenchymal tract. Others have speculated that true duplication may be identified radiologically only when hydromyelia is detected within each "hemicord", as this implies complete duplication of the central ependymal canal and, therefore, of the surrounding spinal cord (C. Raybaud, personal communication); however, nonhydromyelic hemicords have also necessarily completed their neurulation (and therefore possess an undilated central canal), otherwise a hemimyelo(meningo)cele would result from lack of neurulation of one hemicord. In other words, all spinal cords would be duplicated if successful neurulation of both hemicords is taken as a standpoint.

Analysing our 24 cases of SCM and reviewing the pertinent literature we have come to the conclusion that there is a continuous spectrum of abnormality ranging from a partially cleft spinal cord in a single dural tube at one end to a completely duplicated cord within dual dural tubes with an intervening bony spur at the other; if this is so, the dispute as to whether the spinal cord is cleft or duplicated would lose its meaning, and we tend to call all these cases "diastematomyelia" in everyday language. However, we agree with the scheme devised by Pang et al. [19] because it provides a classification based on reproducible observations, although it should be borne in mind that single dural tube SCM (type II) may produce cord tethering cord if an intervening fibrous septum is present.

In conclusion, diastematomyelia and diplomyelia are two ends of a spectrum of split-cord malformations with a common embryonic mechanism. In both cases, the two hemicords are in fact "incomplete duplications", with relatively well-preserved lateral halves and dystrophic medial halves representing a variable degree of duplication. Both hemicords usually attain complete neurulation, as demonstrated by the presence of a continuous cutaneous covering of the malformation and, sometimes, by the recognition of the ependymal canal within the hemicords. Failure of neurulation results in a hemimyelo(meningo)cele.

Dermal sinus

The dermal sinus is an epithelium-lined fistula which extends inwards from the skin surface and sometimes connects with the central nervous system and its meningeal coating. It is found more frequently in the lumbosacral region, although cervical and thoracic sinuses are possible [62]; it is very common (23.7 % of CSD in our series). On examination, a midline dimple or pinpoint ostium is found, often with a hairy naevus, capillary haemangioma or hyperpigmented patches. A dermal sinus must be differentiated from the dimple of a

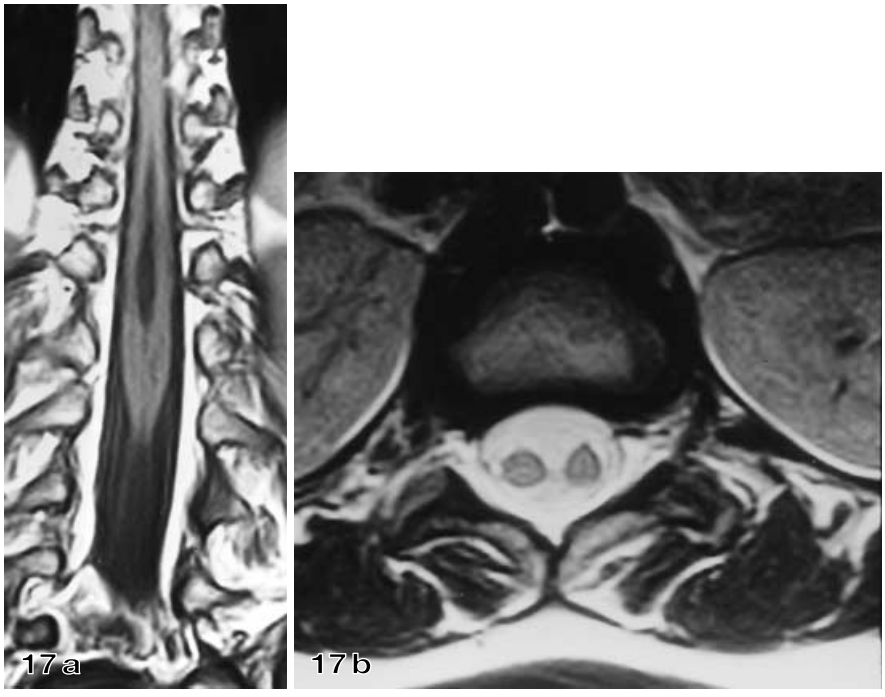

Fig. 17a, b Type II split cord malformation (diastematomyelia without septum). **a** Coronal T1-weighted image shows thoracolumbar split cord. However, this could represent a persistent terminal ventricle. **b** Axial T2-weighted image clearly shows the two hemicords in a single dural tube, with no intervening spur

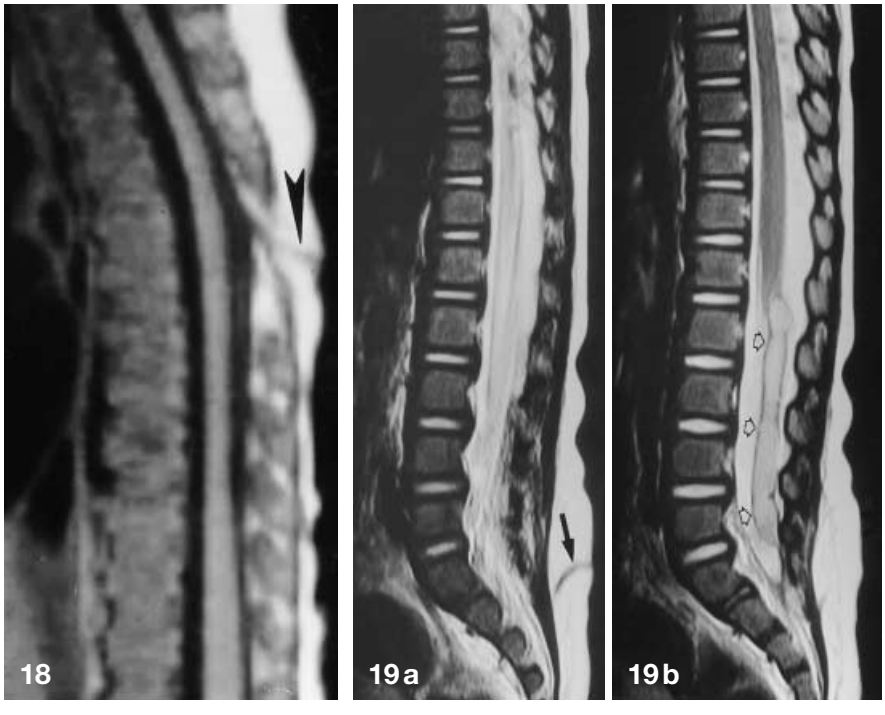

Fig. 18 Dermal sinus. Sagittal T1-weighted image shows thoracic dermal sinus coursing slightly upwards to connect with the spinal canal *(arrowhead).* CSF was seen leaking from a cutaneous pinpoint ostium

Fig. 19a, b Dermal sinus with dermoid. **a** Slightly parasagittal T2-weighted image shows sacral dermal sinus coursing obliquely downwards in subcutaneous fat *(arrow).* **b** Midsagittal image shows a huge dermoid in the thecal sac *(open arrows),* extending upwards to the tip of the conus medullaris. The mass gives slightly lower signal than CSF and is outlined by a thin low-signal rim

pilonidal sinus, which is generally near the anus and does not communicate with the spinal canal.

Embryologically, dermal sinus tracts have traditionally been believed to result from focal incomplete disjunction of the neuroectoderm from the cutaneous ectoderm [63]. However, this theory has been questioned [3]: the dermal sinus could derive from ectodermal differentiation of the dorsal portion of the neurenteric canal; it could thus be isolated or associated with split-cord malformations, depending on the severity of the malformation.

Dermal sinuses may open in the subarachnoid space, causing leakage of CSF, or be connected to a hypertrophic or fibrolipomatous filum terminale, a low conus

medullaris or intraspinal lipoma. They also may originate from the skin overlying a lipomyeloschisis, which is therefore pierced by the dermal sinus. Generally, the sinus courses obliquely and downwards, and is easily recognised on midline sagittal images as a thin low-signal stripe in the subcutaneous fat (Fig. 18); it is more difficult to detect on axial images. Ascending meningitis is a recognised complication of sinuses connecting with the intradural space [63]. In a considerable percentage of cases, the sinus is associated with a dermoid, generally at the level of the cauda equina, or near the conus medullaris (Fig. 19). This association was found in 11.3 % of our cases. The dermoid probably results from encystment of part of the dermal sinus tract and may increase in size due to progressive accumulation of desquamative debris within the cyst. Abscess formation and rupture into the subarachnoid space, with consequent chemical meningitis, are other well-recognised complications of spinal dermoids [63].

Disorders of notochord formation. As was previously stated, it is today clear that the eventual location of each prospective notochordal cell along the longitudinal embryonic axis is genetically programmed under control of Homeobox genes; the embryo therefore has a genetically encoded segmental organisation. Programmed cell death, *apoptosis,* is a process of cell elimination which occurs in the course of normal development, and is crucial during various steps of embryogenesis [64]. During gastrulation, cells wrongly specified in terms of their rostrocaudal position are eliminated ("positional apoptosis") [65], so that fewer cells or even no cells at all will form the notochord or caudal cell mass depending on the segmental level of the abnormality. The consequences of this segmental chorda-mesodermal paucity are manifold, and affect development of the spinal column and cord and other organs which rely on the notochord as inductor. If the prospective notochord or caudal cell mass is depopulated, a wide array of segmental vertebral malformations, including segmentation defects, indeterminate or block vertebrae, or even absence of several vertebrae, will result. Moreover, because of lack of neural induction, fewer prospective neuroectodermal cells, or even no cells at all, will be induced to form the neural plate or the secondary neural tube in the pathological segment [23]. The resulting malformation depends essentially on the segmental level and the extent of the abnormality along the longitudinal axis [23]. In the vast majority of cases, the abnormality involves the caudal end of the embryo (i. e., the caudal cell mass and a variable extent of notochord) resulting in the caudal regresssion constellation; much more rarely an intermediate notochordal segment is involved, and segmental spinal dysgenesis results [23]. Isolated vertebral abnormalities such as hemivertebrae or isolated butterfly vertebrae may also be caused by minor notochordal derangement but, as spinal dysraphism is usually not associated with these conditions, they will not be discussed further.

Caudal regression syndrome (CRS)

This is a heterogeneous constellation of caudal anomalies comprising total or partial agenesis of the spinal column, anal imperforation, genital anomalies, bilateral renal dysplasia or aplasia and pulmonary hypoplasia [66]. The lower limbs are usually dysplastic with distal atrophy and a short intergluteal cleft; fusion or agenesis results in the most severe cases (sirenomelia) [67]. Agenesis of the sacrococcygeal spine may be part of syndromic complexes such as OEIS [40], VACTERL (vertebral abnormality, anal imperforation, tracheoesophageal fistula, renal abnormalities, limb deformities) [68], and the Currarino triad (partial sacral agenesis, anorectal malformation and sacrococcygeal teratoma) [69–71]. Lipomyelomeningocele and terminal myelocystocele are present in 20 % of cases [5]. There is an association with maternal diabetes mellitus (1 % of offspring of diabetic mothers being affected) [5]. Overall, CRS is not uncommon, and we saw 103 cases (16.3 % of CSD).

MRI shows two distinct types of abnormality depending on the position of the conus medullaris, which in turn depends on the severity of the malformation [72, 73]. The embryological watershed between the two varieties is the junction between the notochord and caudal cell mass, corresponding to the caudal end of the future neural plate (interface between neural tube closure site 5 and secondary neurulation) [8]. The exact location of such site is the source of continuing debate. Some workers place it at S1–2 [8], others at S3–5 [6]. In practical terms, the difference is negligible, as the sacral and coccygeal metameres of the spinal cord are represented by the tip of the conus medullaris.

Type I. If the derangement is severe (spine ending at S1 or above), the corresponding metameres of the spinal cord will also be absent. This results in a high-lying terminal spinal cord, abrupt (without the normal taper), which is nearly always club-shaped (extending lower dorsally) (Fig. 20) [5, 74]. The higher the cord terminates, the more severe the malformation, with more absent vertebrae. In the most severe cases, there is absence of all coccygeal, sacral, lumbar and some of the thoracic vertebrae and the spinal cord terminates at the midthoracic level. The cauda equina is also frequently abnormal, and the nerve roots have an abnormal course, termed the "double bundle" [72]. Caudal anomalies, such as anterior meningocele, may be found.

Type II. With minor degree of dysgenesis (S2 or lower levels present) only the most caudal part of the conus medullaris (corresponding to the metameres formed by secondary neurulation) is absent; in the vast

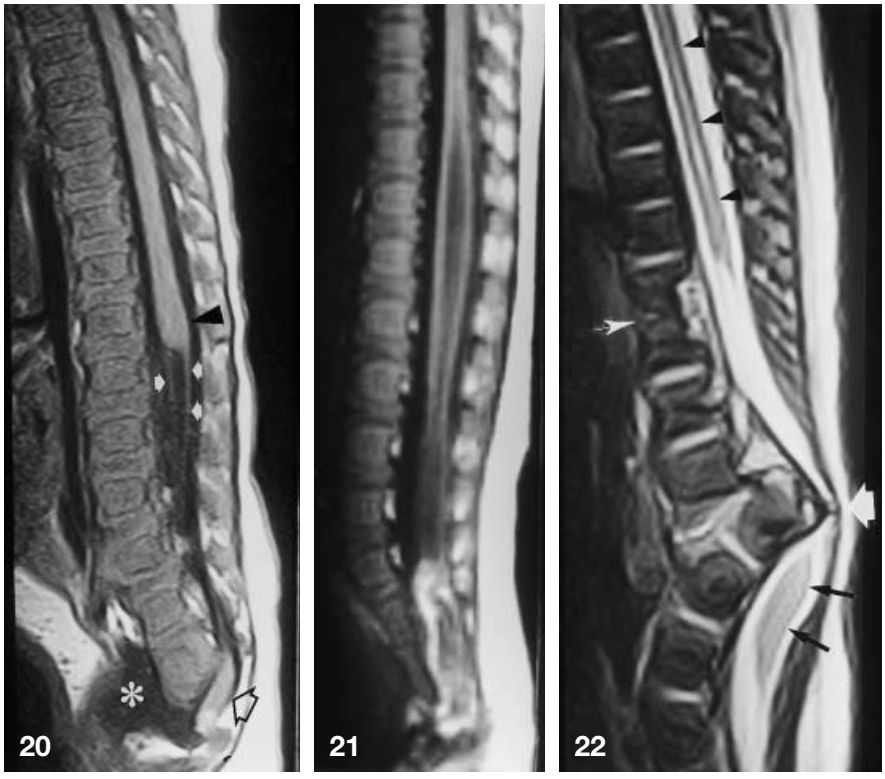

Fig. 20 Caudal regression syndrome, type I. Sagittal T1-weighted image shows complete sacococcygeal agenesis. There is a high, abrupt termination of the spinal cord, extending slightly lower dorsally than ventrally *(black triangle)*. Note "double bundle" shape of the nerve roots of the cauda equina *(white arrows)*. Associated caudal anomalies include anterior meningocele *(asterisk)* and a histologically proven hamartoma *(open arrow)*

Fig. 21 Caudal regression syndrome, type II. Sagittal T1-weighted image shows a lesser degree of sacrococcygeal agenesis than in type I, S3 being present. The spinal cord is tethered to a sacral intradural lipoma and there is a huge hydromyelic cavity

Fig. 22 Segmental spinal dysgenesis. Sagittal T2-weighted image shows an acute thoracolumbar kyphosis with complete interruption of the spinal column and lower thoracic vertebral segmentation defect *(arrow)*. There are two completely separated spinal cord segments; the upper ends several vertebral levels above the gibbus and shows central high signal *(triangles)*, whereas the lower is bulky, low and does not show significant signal change *(black arrows)*. Note extreme narrowing of spinal canal at the affected level *(white arrow)*

majority of cases, the conus is elongated and stretched caudally, and tethered by a tight filum terminale, intradural lipoma (Fig. 21), terminal myelocystocele or lipomyelomeningocele [5]. In some cases, the cord tapers progressively to attach to the neck of an anterior sacral meningocele; the anomaly may be discovered in later childhood or adolescence, when the patient develops constipation, urinary incontinence, dysmenorrhoea, dyspareunia or back pain [5].

In a minority of cases, cord tethering is not present, and only the tip of the conus medullaris is absent; in such cases analysis of both plain films and MRI is required so as not to overlook the abnormality.

Segmental spinal dysgenesis

The clinicoradiological definition of segmental spinal dysgenesis (SSD) includes segmental agenesis or dysgenesis of the lumbar or thoracolumbar spine; segmental abnormality of the underlying spinal cord and nerve roots; congenital paraplegia or paraparesis; and congenital lower limb deformities [23]. Segmental vertebral anomalies may involve the thoracolumbar, lumbar, or lumbosacral spine. The spinal cord may be hypoplastic or completely absent at level of the abnormality, depending on the severity of the causal insult, while a bulky, low-lying lower cord segment is present caudal to the focal abnormality, to the extent that the spine and spinal cord are "cut in two" in the most severe cases (Fig. 22) [23]. Other CSD, partial sacrococcygeal agenesis, and renal abnormalities may be present.

Although SSD is a specific entity showing particular clinical and neuroradiological features, SSD and CRS probably represent two parts of a single spectrum of segmental malformations of the spine and spinal cord, the main difference being the level of the causal notochordal derangement along the longitudinal embryonic axis [23]. As with CRS, the embryogenesis of SSD could be due to genetically induced notochordal derangement during gastrulation, resulting in depopulation of the prospective neuroectoderm [23]. However, if one considers that the CRS/SSD ratio in our series is 11 : 1, it becomes clear that the caudal extremity of the embryo must be far more susceptible than intermediate segments to damage during early embryonic development. In SSD, the neuroradiological picture depends on the severity of the malformation and on its level along

the longitudinal axis. The severity of the morphological derangement correlates with residual spinal cord function and the severity of the clinical deficit [23].

Conclusion

We have tried to devise an analytical approach to imaging children with spinal dysraphism which may prove useful in everyday clinical practice. As with other disease processes, the initial step is clinical, and the neuroradiologist should not refrain from carefully examining a child's back, as this is one of the most crucial points to a correct diagnosis. MRI has replaced other imaging techniques, with the possible exception of CT for characterising the spur in split-cord malformations. In most instances, sagittal, axial, and coronal T1-weighted images will suffice. Fast spin-echo T2-weighted images are especially useful when looking for complications of cord tethering such as hydromyelia. The most challenging cases are probably split-cord malformations, which may require a three-plane examination with both T1- and T2-weighted images. However, plain films in anteroposterior and lateral projections are still mandatory for assessing associated abnormalities of the spinal column. Close interdisciplinary collaboration involving neuroradiologists, neurosurgeons, paediatricians, orthopaedic surgeons, physical therapists, urologists and psychologists is required to provide these patients with treatment tailored to their individual needs.

References

1. Auroux M, Haegel P (1992) Organogenése. Système nerveux, organes de sens, intégration neuro-endocrinienne. In: Tuchmann-Duplessis H (ed) Embryologie. Travaux pratiques et enseignement dirigé, 3rd edn. Masson, Paris, vol 3
2. Bayer SA, Altman J, Russo RJ, Zhang X (1995) Embryology. In: Duckett S (ed) Pediatric neuropathology. Williams & Wilkins, Baltimore, pp 54–107
3. Dias MS, Walker ML (1992) The embryogenesis of complex dysraphic malformations: a disorder of gastrulation? Pediatr Neurosurg 18: 229–253
4. Moore KL (ed) (1988) The developing human. Clinically oriented embryology, 4th edn. Saunders, Philadelphia
5. Naidich TP, Zimmerman RA, McLone DG, Raybaud CA, Altman NR, Braffman BH (1996) Congenital anomalies of the spine and spinal cord. In: Atlas SW (ed) Magnetic resonance imaging of the brain and spine, 2nd edn. Lippincott-Raven, Philadelphia, pp 1265–1337
6. Nievelstein RAJ, Hartwig NG, Vermeji-Keers C, Valk J (1993) Embryonic development of the mammalian caudal neural tube. Teratology 48: 21–31
7. Raybaud CA, Naidich TP, McLone DG (1992) Development of the spine and spinal cord. In: Manelfe C (ed) Imaging of the spine and spinal cord. Raven Press, New York, pp 93–113
8. Van Allen MI, Kalousek DK, Chernoff GF, Juriloff D, Harris M, McGillivray BC, Yong SL, Langlois S, MacLeod PM, Chitayat D, Friedman JM, Wilson RD, McFadden D, Pantzar J, Ritchie S, Hall JG (1993) Evidence for multisite closure of the neural tube in humans. Am J Med Genet 47: 723–743
9. Drolet B (1998) Birthmarks to worry about. Cutaneous markers of dysraphism. Dermatol Clin 16: 447–453
10. French BN (1983) The embryology of spinal dysraphism. Clin Neurosurg 30: 295–340
11. Sattar MT, Bannister CM, Turnbull IW (1996) Occult spinal dysraphism – The common combination of lesions and the clinical manifestations in 50 patients. Eur J Pediatr Surg 6 [Suppl 1]: 10–14
12. Tortori-Donati P, Fondelli MP, Rossi A (1998) Anomalie congenite del midollo spinale. In: Simonetti G, Del Maschio A, Bartolozzi C, Passariello R (eds) Trattato italiano di risonanza magnetica. Idelson-Gnocchi, Naples, pp 517–553
13. Herman JM, McLone DG, Storrs BB, Dauser RC (1993) Analysis of 153 patients with myelomeningocele or spinal lipoma reoperated upon for a tethered cord. Pediatr Neurosurg 19: 243–249
14. McLone DG, Dias MS (1991–92) Complications of myelomeningocele closure. Pediatr Neurosurg 17: 267–273
15. Tortori-Donati P, Cama A, Rosa ML, Andreussi L, Taccone A (1990) Occult spinal dysraphism: neuroradiological study. Neuroradiology 31: 512–522
16. Raghavan N, Barkovich AJ, Edwards M, Norman D (1989) MR imaging in the tethered spinal cord syndrome. AJNR 10: 27–36
17. Long FR, Hunter JV, Mahboubi S, Kalmus A, Templeton JM (1996) Tethered cord and associated vertebral anomalies in children and infants with imperforate anus: evaluation with MR imaging and plain radiography. Radiology 200: 377–382
18. Scott RM, Wolpert SM, Bartoshesky LF, Zimbler S, Klauber GT (1986) Dermoid tumors occurring at the site of previous myelomeningocele repair. J Neurosurg 65: 779–783
19. Pang D, Dias MS, Ahab-Barmada M (1992) Split cord malformation. I. A unified theory of embryogenesis for double spinal cord malformations. Neurosurgery 31: 451–480
20. Pang D (1992) Split cord malformation. II. Clinical syndrome. Neurosurgery 31: 481–500
21. Cama A, Tortori-Donati P, Piatelli GL, Fondelli MP, Andreussi L (1995) Chiari complex in children. Neuroradiological diagnosis, neurosurgical treatment and proposal of a new classification (312 cases). Eur J Pediatr Surg 5 [Suppl 1]: 35–38
22. Tortori-Donati P, Cama A, Fondelli MP, Rossi A (1996) Le malformazioni di Chiari. In: Tortori-Donati P, Taccone A, Longo M (eds) Malformazioni cranio-encefaliche. Neuroradiologia. Minerva Medica, Turin, pp 209–236
23. Tortori-Donati P, Fondelli MP, Rossi A, Raybaud CA, Cama A, Capra V (1999) Segmental spinal dysgenesis. Neuroradiologic findings with clinical and embryologic correlation. AJNR 20: 445–456
24. Smithells RW, Sheppard S, Schorah CJ, Seller MJ, Nevin NC, Harris R, Read AP, Fielding DW (1980) Possible prevention of neural tube defects by periconceptional vitamin supplementation. Lancet i: 339–340
25. McLone DG, Knepper PA (1985–86) Role of complex carbohydrates and neurulation. Pediatr Neurosci 12: 2–9
26. Pang D, Dias MS (1993) Cervical myelomeningoceles. Neurosurgery 33: 363–373
27. Breningstall GN, Marker SM, Tubman DE (1992) Hydrosyringomyelia and diastematomyelia detected by MRI in myelomeningocele. Pediatr Neurol 8: 267–271
28. McLone DG, Knepper PA (1989) The cause of Chiari II malformation: a unified theory. Pediatr Neurosci 15: 1–12
29. Naidich TP, McLone DG, Fulling F (1983) The Chiari II malformation. Part IV. The hindbrain deformity. Neuroradiology 25: 179–197

30. Naidich TP, McLone DG, Mutleur S (1983) A new understanding of dorsal dysraphism with lipoma (lipomyeloschisis): radiological evaluation and surgical correlation. AJNR 4: 103–116
31. Pierre-Kahn A, Zerah M, Renier D, Cinalli G, Sainte-Rose C, Lellouch-Tubiana A, Brunelle F, Le Merrer M, Giudicelli Y, Pichon J, Kleinknecht B, Nataf F (1997) Congenital lumbosacral lipomas. Child's Nerv Syst 13: 298–334
32. Knittle JL, Timmers K, Ginsberg-Fellner F, Brown RE, Katz DP (1979) The growth of adipose tissue in children and adolescents. Cross-sectional and longitudinal studies of adipose cell number and size. J Clin Invest 63: 239–246
33. Raimondi AJ (1989) Hamartomas and the dysraphic state. In: Raimondi AJ, Choux M, Di Rocco C (eds) The pediatric spine I. Development and the dysraphic state. Springer, Berlin, pp 179–199
34. Lee KS, Gower DJ, McWhorter JM, Albertson DA (1988) The role of MR imaging in the diagnosis and treatment of anterior sacral meningocele. Report of 2 cases. J Neurosurg 69: 628–631
35. Castillo M, Mukherji SK (1996) Imaging of the pediatric head, neck, and spine. Lippincott-Raven, Philadelphia, pp 638–640
36. Okada T, Imae S, Igarashi S, Koyama T, Yamashita J (1996) Occult intrasacral meningocele associated with spina bifida: a case report. Surg Neurol 46: 147–149
37. Byrd SE, Harvey C, Darling CF (1995) MR of terminal myelocystoceles. Eur J Radiol 20: 215–220
38. McLone DG, Naidich TP (1985) Terminal myelocystocele. Neurosurgery 16: 36–43
39. Peacock WJ, Murovic JA (1989) Magnetic resonance imaging in myelocystoceles. Report of two cases. J Neurosurg 70: 804–807
40. Carey JC, Greenbaum B, Hall BD (1978) The OEIS complex (omphalocele, exstrophy, imperforate anus, spinal defects). Birth Defects Orig Artic Ser 14: 253–263
41. Smith NM, Chambers HM, Furness ME, Haan EA (1992) The OEIS complex omphalocele-exstrophy-imperforate anus-spinal defects: recurrence in sibs. J Med Genet 29: 730–732
42. Bhargava R, Hammond DI, Benzie RJ, Carlos E, Ventureyra G, Higgins MJ, Martin DJ (1992) Prenatal demonstration of a cervical myelocystocele. Prenat Diagn 12: 653–659
43. McComb JG (1993) Comment on: Pang D, Dias MS. Cervical myelomeningoceles. Neurosurgery 33: 373
44. Parent AD (1993) Comment on: Pang D, Dias MS. Cervical myelomeningoceles. Neurosurgery 33: 372–373
45. Altman NR, Altman DH (1987) MR imaging of spinal dysraphism. AJNR 8: 533–538
46. Hendrick EB, Hoffman HJ, Humphreys RP (1983) The tethered spinal cord. Clin Neurosurg 30: 457–463
47. Uchino A, Mori T, Ohno M (1991) Thickened fatty filum terminale: MR imaging. Neuroradiology 33: 331–333
48. Yundt KD, Park TS, Kaufman BA (1997) Normal diameter of filum terminale in children: in vivo measurement. Pediatr Neurosurg 27: 257–259
49. Kernohan JW (1924) The ventriculus terminalis: its growth and development. J Comp Neurol 38: 10–125
50. Coleman LT, Zimmerman RA, Rorke LB (1995) Ventriculus terminalis of the conus medullaris: MR findings in children. AJNR 16: 1421–1426
51. Sigal R, Denys A, Halimi P, Shapeero L, Doyon D, Boudghène F (1991) Ventriculus terminalis of the conus medullaris: MR imaging in four patients with congenital dilatation. AJNR 12: 733–737
52. Prop N, Frensdorf EL (1967) A postvertebral endodermal cyst associated with axial deformities: a case showing the "endodermal-ectodermal adhesion syndrome". Pediatrics 39: 555–562
53. Faris JC, Crowe JE (1975) The split notochord syndrome. J Pediatr Surg 10: 467–472
54. Hoffman CH, Dietrich RB, Pais MJ, Demos DS, Pribham HFW (1993) The split notochord syndrome with dorsal enteric fistula. AJNR 14: 622–627
55. Castillo M, Hankins L, Kramer L, Wilson BA (1992) MR imaging of diplomyelia: case report. Magn Reson Imaging 10: 699–703
56. Brooks BS, Duvall ER, El Gammal T, Garcia JH, Gupta KL, Kapila A (1993) Neuroimaging features of neurenteric cysts: analysis of nine cases and review of the literature. AJNR 14: 735–746
57. Gao P, Osborn AG, Smirniotopoulos JG, Palmer CA, Boyer RS (1995) Neurenteric cysts. Pathology, imaging spectrum, and differential diagnosis. Int J Neuroradiol 1: 17–27
58. Kincaid PK, Stanley P, Kovanlikaya A, Mahour GH, Rowland JM (1999) Coexistent neurenteric cyst and enterogenous cyst. Further support for a common embryologic error. Pediatr Radiol 29: 539–541
59. Naidich TP, Harwood-Nash DC (1983) Diastematomyelia. Part I. Hemicords and meningeal sheaths. Single and double arachnoid and dural tubes. AJNR 4: 633–636
60. Schlesinger AE, Naidich TP, Quencer RM (1986) Concurrent hydromyelia and diastematomyelia. AJNR 7: 473–477
61. Scotti G, Harwood-Nash DC (1980) Congenital thoracic dermal sinus: diagnosis by computer assisted metrizamide myelography. J Comput Assist Tomogr 4: 675–677
62. Barkovich AJ, Edwards MSB, Cogen PH (1991) MR evaluation of spinal dermal sinus tracts in children. AJNR 12: 123–129
63. Ersahin Y, Mutluer S, Kocaman S, Demirtas E (1998) Split spinal cord malformations in children. J Neurosurg 88: 57–65
64. Wyllie AH (1987) Apoptosis: cell death in tissue regulation. J Pathol 153: 313–316
65. Maden M, Graham A, Gale E, Rollinson C, Zile M (1997) Positional apoptosis during vertebrate CNS development in the absence of endogenous retinoids. Development 124: 2799–2805
66. Duhamel B (1961) From the mermaid to anal imperforation: the syndrome of caudal regression. Arch Dis Child 36: 152–155
67. Valenzano M, Paoletti R, Rossi A, Farinini D, Garlaschi G, Fulcheri E (1999) Sirenomelia. Pathological features, antenatal ultrasonographic clues, and a review of current embryogenic theories. Hum Reprod Update 5: 82–86
68. Raffel C, Litofsky S, McComb JG (1990–91) Central nervous system malformations and the VATER association. Pediatr Neurosurg 16: 170–173
69. Currarino G, Coln D, Votteler T (1981) Triad of anorectal, sacral, and presacral anomalies. AJR 137: 395–398
70. Dias MS, Azizkhan RG (1998) A novel embryogenetic mechanism for Currarino's triad: inadequate dorsoventral separation of the caudal eminence from hindgut endoderm. Pediatr Neurosurg 28: 223–229
71. Gudinchet F, Maeder P, Laurent T, Meyrat B, Schnyder P (1997) Magnetic resonance detection of myelodysplasia in children with Currarino triad. Pediatr Radiol 27: 903–907
72. Nievelstein RAJ, Valk J, Smit LME, Vermeji-Keers C (1994) MR of the caudal regression syndrome: embryologic implications. AJNR 15: 1021–1029
73. Pang D (1993) Sacral agenesis and caudal spinal cord malformations. Neurosurgery 32: 755–779
74. Barkovich AJ, Raghavan N, Chuang SH (1989) MR of lumbosacral agenesis. AJNR 10: 1223–1231